AD NUMBER

AD872813

LIMITATION CHANGES

TO:

Approved for public release; distribution is unlimited.

FROM:

Distribution authorized to U.S. Gov't. agencies and their contractors; Critical Technology; JUL 1970. Other requests shall be referred to U.S. Army Aviation Materiel Laboratories , Fort Eustis , Virginia 23604. This document contains export-controlled technical data.

AUTHORITY

USAAMRDL ltr, 23 Jun 1971

AD

19

USAAVLABS TECHNICAL REPORT 69-82

NONLINEAR FREE VIBRATIONS OF THIN, CIRCULAR CYLINDRICAL SHELLS

By

J. Mayers

B. G. Wrenn

July 1970

U. S. ARMY AVIATION MATERIEL LABORATORIES
FORT EUSTIS, VIRGINIA

CONTRACT DA 44-177-AMC-115(T)
DEPARTMENT OF AERONAUTICS AND ASTRONAUTICS
STANFORD UNIVERSITY
STANFORD, CALIFORNIA

74

Disclaimers

The findings in this report are not to be construed as an official Department of the Army position unless so designated by other authorized documents.

When Government drawings, specifications, or other data are used for any purpose other than in connection with a definitely related Government procurement operation, the United States Government thereby incurs no responsibility nor any obligation whatsoever; and the fact that the Government may have formulated, furnished, or in any way supplied the said drawings, specifications, or other data is not to be regarded by implication or otherwise as in any manner licensing the holder or any other person or corporation, or conveying any rights or permission, to manufacture, use, or sell any patented invention that may in any way be related thereto.

Disposition Instructions

Destroy this report when no longer needed. Do not return it to the originator.

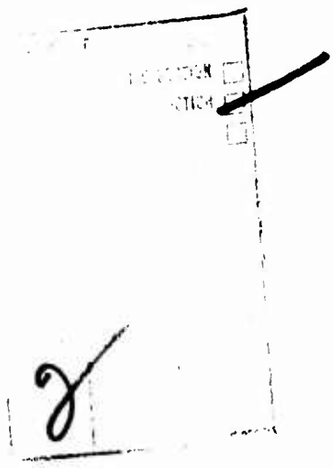

DEPARTMENT OF THE ARMY
HEADQUARTERS US ARMY AVIATION MATERIEL LABORATORIES
FORT EUSTIS, VIRGINIA 23604

This program was carried out under Contract DA 44-177-AMC-115(T) with Stanford University.

The data contained in this report are the result of research conducted to evaluate the influence of higher order and nonlinear effects on the free vibration behavior of thin, circular cylindrical shells.

The report has been reviewed by the U.S. Army Aviation Materiel Laboratories and is considered to be technically sound. It is published for the exchange of information and the stimulation of future research.

Task 1F162204A17002
Contract DA 44-177-AMC-115(T)
USAAVLABS Technical Report 69-82
July 1970

NONLINEAR FREE VIBRATIONS OF THIN, CIRCULAR CYLINDRICAL SHELLS

by

J. Mayers and B. G. Wrenn

Prepared by

Stanford University
Department of Aeronautics and Astronautics
Stanford, California

for

U. S. ARMY AVIATION MATERIEL LABORATORIES
FORT EUSTIS, VIRGINIA

SUMMARY

This report presents the results of a study of the influence of higher order and nonlinear effects on the free vibration behavior of thin, circular cylindrical shells. A recent solution utilizing the Karman-Donnell strain-displacement relations is examined and criticized. A new solution is carried out which removes the basis for criticism and discloses the existence of a nonperiodic vibration behavior, a phenomenon heretofore unknown. Further, solutions are obtained using the strain-displacement relations deduced by Sanders and applied, in an appropriately modified manner, by Mayers and Rehfield to the shell postbuckling problem. The effect of the improved strain-displacement relations in predicting the vibration behavior attendant to a modal shape possessing a small number of circumferential waves is assessed, and recommendations are made for directing future effort on the problem.

TABLE OF CONTENTS

LIST OF ILLUSTRATIONS

LIST OF SYMBOLS

c	Speed of sound in shell material, $(c^2 \equiv E/\rho)$
D	Flexural stiffness, $D \equiv \frac{Eh^3}{12(1-\nu^2)}$
E	Young's modulus of elasticity
F	Airy stress function
h	Uniform wall thickness of the shell
ℓ	Cylinder length
L	Lagrangian, $(L \equiv T - U)$
$\bar{L}$	Nondimensional Lagrangian parameter, $\left[\bar{L} \equiv \left(\frac{\pi Eh^3 \ell}{R}\right)^{-1} L\right]$
M_x, M_y	Bending moments per unit length
M_{xy}	Twisting moment per unit length
m	Number of axial full waves in the modal pattern
n	Number of circumferential full waves in the modal pattern
Q_x, Q_y	Shearing forces per unit length
R	Mean radius of the circular cylindrical shell
t	Time
T	Kinetic energy
U	Strain energy

$\bar{U}$	Nondimensional strain energy parameter, $\left[\bar{U} \equiv \left(\frac{\pi E h^3 \ell}{R}\right)^{-1} U\right]$
u_t, v_t, w_t	Components of the midsurface displacement in the axial, tangential, and radial directions, respectively
u, v, w	Components of the midsurface displacement in the axial, circumferential, and radial directions, respectively
x, θ, z	Coordinates shown in Figure 1
y	$= R\theta$
$y_i(t)$	Arbitrary functions of time ($i = 1,2,3\ldots$)
γ_{xy}	Shearing strain
γ^0_{xy}	Midsurface shearing strain
ϵ_x, ϵ_y	Extensional strains
$\epsilon^0_x, \epsilon^0_y$	Midsurface extensional strains
η	Wave parameter, $\left[\eta \equiv n^2 \left(\frac{h}{R}\right)\right]$
$\kappa_x, \kappa_y, \kappa_{xy}$	Changes in curvature and twist of the shell midsurface
λ_x	Half wavelength in the axial direction, $(\lambda_x \equiv \frac{\ell}{2m})$
λ_y	Half wavelength in the circumferential direction, $(\lambda_y \equiv \frac{\pi R}{n})$
μ	Full wave aspect ratio, $\left(\mu \equiv \frac{2\lambda_y}{2\lambda_x}\right)$
ν	Poisson's ratio

ρ — Mass density of the shell material

σ_x, σ_y — Extensional stresses

σ_x^0, σ_y^0 — Midsurface extensional stresses

τ_{xy} — Shearing stress

τ_{xy}^0 — Midsurface shearing stress

τ — Nondimensional independent variable, $\left[\tau \equiv \left(\frac{c}{R}\right) t\right]$

Φ_x, Φ_y — Angles of rotation defined in Equations (4) and (5)

ω — Frequency

$\omega_{K\text{-}D}$ — Frequency based on use of the Karman-Donnell theory

ω_S — Frequency based on use of the Sanders theory

ω_L — Frequency for linear theory (see Reference 8),

$$\omega_L^2 \equiv \frac{E}{\rho R^2}\left[\frac{\mu^4}{(1+\mu^2)^2} + \frac{\eta^2(1+\mu^2)^2}{12(1-\nu^2)}\right]$$

$(\omega_S)_L$ — Frequency based on the use of the linearized Sanders theory

OPERATOR SYMBOLS

$$\nabla^2(\ ) = \frac{\partial^2(\ )}{\partial x^2} + \frac{\partial^2(\ )}{\partial y^2}$$

$$\nabla^4(\ ) = \frac{\partial^4(\ )}{\partial x^4} + 2\frac{\partial^4(\ )}{\partial x^2 \partial y^2} + \frac{\partial^4(\ )}{\partial y^4}$$

INTRODUCTION

In the past, the problem of the instability of thin, circular cylindrical shells subjected to a variety of loadings has been the object of intense theoretical and experimental investigation. A closely allied problem, that of the vibrations of thin, circular cylindrical shells, has also come under careful scrutiny, but not to the same extent nor with the apparent success relative to the instability problem.

The studies related to the vibrating cylindrical shell problem have, for the most part, been contained within the framework of linear theory. Notable contributions to the early development of the vibrating cylindrical shell problem are contained in the work of Rayleigh,[1] Love,[2] Flügge,[3] and Arnold and Warburton.[4,5] A relatively small amount of work has been accomplished concerning the vibrational characteristics outside the realm of linear theory with the well-known Karman-Donnell equations. To assess the merit of this work and to place the present investigation in proper perspective, it is pertinent to dwell somewhat on that part of the literature which deals specifically with the free nonlinear vibrations of thin, circular cylindrical shells.

The first significant step toward the understanding and solution of the nonlinear problem emanated from the work of Eric Reissner[6] in 1955. This paper, although restricted to the linear theory of thin, shallow elastic shells, was the first to show that for vibration in which the predominant motion is radial, the equations of motion admit an important simplification. Specifically, for predominately radial motion of shallow shells, Reissner[6] shows that the midsurface inertia terms (that is, the inertia terms due to motion in the axial and circumferential directions) can be neglected and only minor errors will result. Then, the three coupled simultaneous differential equations of motion can be simplified to a system of two simultaneous differential equations with the dependent variables being the well-known Airy stress function and the radial displacement. This latter set of two coupled differential equations, independent of radial inertia considerations, becomes the well-known equations governing the static instability problem of thin, circular cylindrical shells. The basis for

this simplified set of equations governing the phenomena of static instability is contained in an investigation by Donnell.[7] The work of Donnell,[7] complementary to the classical large deflection theory of flat plates, is generally referred to today as the Karman-Donnell shell theory.

Later in 1955, Reissner[8] published a paper, utilizing shallow shell theory, dealing with both the linear and nonlinear nonaxisymmetric vibrations of thin, circular cylindrical shells. The portion of the work pertaining to the linear theory specializes the earlier work of Reissner[6] to the geometry peculiar to a thin, circular cylindrical shell. For infinitesimal deflections, Reissner assumes that the radial displacement function is representable as a chessboard pattern. That this assumption is valid is strongly substantiated by the experimental evidence of Arnold and Warburton,[4,5] Gottenberg,[9] and most recently by Koval and Cranch[10] and Koval.[11] In the last-noted reference of Koval,[11] no mention is made of comparison to linear theory, but a straightforward calculation shows that the experimental results are almost identical to those obtained using the frequency equation derived by Reissner.[8] In the nonlinear portion of Reissner's study,[8] it is assumed that the nonlinearity has a more pronounced effect on the arbitrary time function, which modifies the choice of deflected shape, than on the deflected shape itself. Hence, the chessboard shape is used also for the nonlinear vibration problem. However, even though the chessboard deflection pattern is a natural choice for linear vibration problems, its selection in the nonlinear problem must be more carefully assessed. In particular, it has been well known in shell postbuckling problems (see, for example, the work of von Karman and Tsien)[12] that the continuity condition on the circumferential displacement must be enforced. This basic geometric constraining requirement must also be employed in the nonlinear shell vibration problem. However, the use of the chessboard pattern leads to a circumferential displacement that is not a periodic function of the circumferential coordinate. Evensen[13] was the first to point out that this continuity requirement was not satisfied by the choice of deflected shape assumed by Reissner.[8]

Another solution, similar to Reissner's,[8] was presented by Chu.[14] Again, as pointed out by Evensen,[13] the continuity requirement for the circumferential displacement was not satisfied. Evensen[13] further notes that in a paper presented by Nowinski,[15] the continuity condition for the circumferential displacement is taken into account; as a consequence, however, a nonzero radial displacement occurs at the ends of the shell. On the other hand, the radial displacement condition utilized by Evensen,[13] as well as by Reissner [8] and Chu,[14] is that of vanishing radial displacement at the shell edges. It should be noted, however, that this difference in the boundary conditions would not likely cause appreciable difference in the vibrating shell problem provided that the modal representation of the deflected shape possessed a large number of axial waves. This latter point is not mentioned by Evensen.[13]

Chu[14] and Nowinski[15] arrived at results which showed that the nonlinear vibrational characteristics of the shell exhibited nonlinearity of the hardening type (that is, an increase in the radial displacement magnitude is shown to lead to an increase in the frequency of radial vibration) which, in some cases, could be strongly nonlinear. These findings were challenged by Evensen,[13] who claimed that the nonlinearity was of the softening type (that is, an increase in the radial displacement magnitude is shown to lead to a decrease in the frequency of radial vibration) and was only slightly nonlinear.

In the latter part of 1965, Evensen and Fulton[16] presented a paper on the nonlinear dynamic response of cylindrical shells which is an expanded version of Evensen's[13] original investigation. Evensen and Fulton[16] arrive at results which modify Evensen's[13] original conclusion (that is, that the shell exhibits either hard or soft behavior depending upon the numerical values of the wavelength parameters attendant to the assumed modal shape). The theoretical results are in agreement with an experiment performed by Olson[17] in 1965. However, the boundary conditions utilized in the work of Evensen and Fulton[16] reflect supported, rotationally restrained ends, whereas the experiment conducted by Olson[17] reflects end clamping.

The objective of the present investigation is to study further the nonlinear free vibrations of thin, circular cylindrical shells on the basis of considerations heretofore excluded from theoretical work appearing in the literature. It is shown that the energy level (potential plus kinetic) associated with a given modal shape is an important consideration in the nonlinear free vibration problem. The initial portion of the study, based upon the Karman-Donnell equations, reveals that the valid solution, corresponding to a modal pattern possessing a large number of axial waves and described in terms of free parameters, is the one that reflects minimum energy considerations, rather than the one that requires the vibration behavior to be periodic. This latter condition is utilized by Evensen and Fulton in Reference 16. It is clearly demonstrated that minimum energy considerations for a free variation of the modal pattern assumed in Reference 16 lead to a nonperiodic motion for the free nonlinear vibrations of thin, circular cylindrical shells. Further, when the number of axial waves in the modal pattern is small and the influence of boundary conditions must be accounted for, the adoption of a more general deflected shape than that employed in Reference 16, but satisfying the same boundary condition, again reveals the existence of a nonperiodic motion. In this latter case, the nonperiodic motion reflects an energy level, for identical initial conditions, equal to that associated with the deflected shape chosen in Reference 16. The nonperiodic motion, in all cases investigated, appears to be almost periodic. This behavior has important implications concerning the interpretation of the results obtained in experimental investigations.

The present study is not limited, as are the previously referenced nonlinear studies, to vibrations where there are a large number of circumferential waves present. That there are a large number of circumferential waves is the basic assumption justifying the utilization of the Karman-Donnell equations. Hence, to surmount the restriction on the use of the Karman-Donnell formulation of the shell problem when the number of circumferential waves is small, it is necessary to employ a more accurate set of strain-displacement relations and, at the same time, to retain the midsurface inertia terms. The observations by Reissner[6,8] that

midsurface inertia terms may be neglected when the number of circumferential waves is large can no longer be invoked.

The more accurate strain-displacement relations employed are attributed to Sanders[18] and were used, in a modified form, by Mayers and Rehfield[19] in a study of the postbuckling characteristics of thin, circular cylindrical shells. As illustrated by Mayers and Rehfield,[19] the postbuckling solutions obtained on the basis of the modified Sanders relations can be utilized to establish the range of validity of elastic, large deflection solutions (specifically, those based on the Karman-Donnell formulation) in terms of shell radius-to-thickness ratio. The ramifications of these findings relative to the nonlinear shell vibration problem are pursued.

Differential equations of motion and the attendant boundary terms are developed on the basis of a variational procedure. Approximate solutions of the equations are obtained, and the results presented clarify former work and yield new information regarding the nonlinear vibrational characteristics of thin, circular cylindrical shells.

THEORETICAL CONSIDERATIONS

STRAIN-DISPLACEMENT RELATIONS

The strain-displacement relations used in this study were deduced by Sanders.[18] For the thin, circular cylindrical shell, the midsurface strains can be reduced to the form

$$\epsilon_x^0 = \frac{\partial u_t}{\partial x} + \frac{1}{2}(\varphi_x)^2 \tag{1}$$

$$\epsilon_y^0 = \frac{\partial v_t}{\partial y} - \frac{w_t}{R} + \frac{1}{2}(\varphi_y)^2 \tag{2}$$

$$\gamma_{xy}^0 = \frac{\partial u_t}{\partial y} + \frac{\partial v_t}{\partial x} + \varphi_x \varphi_y \tag{3}$$

where

$$\varphi_x = -\frac{\partial w_t}{\partial x} \tag{4}$$

$$\varphi_y = -\left(\frac{\partial w_t}{\partial y} + \frac{v_t}{R}\right) \tag{5}$$

The total strains are then given by

$$\epsilon_x = \epsilon_x^0 + z\kappa_x \tag{6}$$

$$\epsilon_y = \epsilon_y^0 + z\kappa_y \tag{7}$$

$$\gamma_{xy} = \gamma_{xy}^0 + 2z\kappa_{xy} \tag{8}$$

where u_t, v_t, and w_t (see Figure 1) are the axial, tangential, and radial components of displacement, respectively, and

$$\kappa_x = \frac{\partial \varphi_x}{\partial x} \; ; \; \kappa_y = \frac{\partial \varphi_y}{\partial y} \; ; \; \kappa_{xy} = \frac{1}{2}\left(\frac{\partial \varphi_x}{\partial y} + \frac{\partial \varphi_y}{\partial x}\right) \tag{9}$$

Substitution of Equations (1) through (5) and (9) into Equations (6) through (8) yields the strain-displacement relations

$$\epsilon_x = \frac{\partial u_t}{\partial x} + \frac{1}{2}\left(\frac{\partial w_t}{\partial x}\right)^2 - z\frac{\partial^2 w_t}{\partial x^2} \tag{10}$$

$$\epsilon_y = \frac{\partial v_t}{\partial y} - \frac{w_t}{R} + \frac{1}{2}\left[\left(\frac{\partial w_t}{\partial y}\right)^2 + 2\frac{v_t}{R}\frac{\partial w_t}{\partial y} + \frac{v_t^2}{R^2}\right] - z\left(\frac{\partial^2 w_t}{\partial y^2} + \frac{1}{R}\frac{\partial v_t}{\partial y}\right) \tag{11}$$

$$\gamma_{xy} = \frac{\partial u_t}{\partial y} + \frac{\partial v_t}{\partial x} + \frac{\partial w_t}{\partial x}\frac{\partial w_t}{\partial y} + \frac{v_t}{R}\frac{\partial w_t}{\partial x} - z\left(2\frac{\partial^2 w_t}{\partial x \partial y} + \frac{1}{R}\frac{\partial v_t}{\partial x}\right) \tag{12}$$

Equations (10), (11), and (12) are valid when (1) the Kirchhoff-Love hypothesis holds (that is, when a straight line segment that is perpendicular to the middle surface of the undeformed shell remains perpendicular to the deformed middle surface while undergoing negligible strain relative to its original length), (2) the strains and rotations of line elements on the shell midsurface induced by the deformation remain small in comparison to unity, although the components of the displacements are not necessarily small, and (3) the angles of rotation about the normals to the shell midsurface remain negligibly smaller than the rotations out of the midsurface throughout the deformation.

Although the Sanders Equations (10), (11), and (12) appear as a displacement formulation in terms of a tangential v-displacement notation, they can be written in terms of a circumferential v-displacement notation to effect a convenient simplification as shown by Mayers and Rehfield.[19] In the alternate form, the equations become

$$\epsilon_x = \frac{\partial u}{\partial x} + \frac{1}{2}\left(\frac{\partial w}{\partial x}\right)^2 - z\frac{\partial^2 w}{\partial x^2} \tag{13}$$

$$\epsilon_y = \frac{\partial v}{\partial y} - \frac{w}{R} + \frac{1}{2}\left[\left(\frac{\partial w}{\partial y}\right)^2 + 2\frac{v}{R}\frac{\partial w}{\partial y}\right] - z\left(\frac{\partial^2 w}{\partial y^2} + \frac{1}{R}\frac{\partial v}{\partial y}\right) \tag{14}$$

and

$$\gamma_{xy} = \frac{\partial v}{\partial x} + \frac{\partial u}{\partial y} + \frac{\partial w}{\partial x}\frac{\partial w}{\partial y} + \frac{v}{R}\frac{\partial w}{\partial x} - z\left(2\frac{\partial^2 w}{\partial x \partial y} + \frac{1}{R}\frac{\partial v}{\partial x}\right) \tag{15}$$

It may be noted that Equations (13), (14), and (15) reflect no quadratic terms in the midsurface displacements alone. Also, for a large number of circumferential waves, the equations can be further simplified by elimination of any v-displacement contributions to the curvatures and twist.

TOTAL POTENTIAL ENERGY

The total potential energy, in the absence of body forces, consists of the strain energy stored in the body and can be expressed as

$$U = \int_0^{\ell}\int_0^{2\pi R}\int_{-h/2}^{+h/2} \frac{E}{2(1-\nu^2)}\left[\epsilon_x^2 + \epsilon_y^2 + 2\nu\epsilon_x\epsilon_y + \frac{(1-\nu)}{2}\gamma_{xy}^2\right] dxdydz \tag{16}$$

Substitution of the expressions for the strains from Equations (13), (14), and (15) into Equation (16) and integration over the constant thickness of the shell yield

$$\begin{aligned} U = {} & \frac{Eh}{2(1-\nu^2)}\int_0^{\ell}\int_0^{2\pi R}\left\{\left[\frac{\partial u}{\partial x} + \frac{1}{2}\left(\frac{\partial w}{\partial x}\right)^2\right]^2 + \left[\frac{\partial v}{\partial y} - \frac{w}{R} + \frac{1}{2}\left(\frac{\partial w}{\partial y}\right)^2 + \frac{v}{R}\frac{\partial w}{\partial y}\right]^2 \right. \\ & + 2\nu\left[\frac{\partial u}{\partial x} + \frac{1}{2}\left(\frac{\partial w}{\partial x}\right)^2\right]\left[\frac{\partial v}{\partial y} - \frac{w}{R} + \frac{1}{2}\left(\frac{\partial w}{\partial y}\right)^2 + \frac{v}{R}\frac{\partial w}{\partial y}\right] + \frac{(1-\nu)}{2}\left[\frac{\partial u}{\partial y}\right. \\ & \left.\left. + \frac{\partial v}{\partial x} + \frac{\partial w}{\partial x}\frac{\partial w}{\partial y} + \frac{v}{R}\frac{\partial w}{\partial x}\right]^2\right\} dxdy + \frac{D}{2}\int_0^{\ell}\int_0^{2\pi R}\left\{\left(\frac{\partial^2 w}{\partial x^2}\right)^2\right. \\ & + \left(\frac{\partial^2 w}{\partial y^2} + \frac{1}{R}\frac{\partial v}{\partial y}\right)^2 + 2\nu\left(\frac{\partial^2 w}{\partial x^2}\right)\left(\frac{\partial^2 w}{\partial y^2} + \frac{1}{R}\frac{\partial v}{\partial y}\right) + \frac{(1-\nu)}{2}\left(2\frac{\partial^2 w}{\partial x \partial y}\right. \\ & \left.\left. + \frac{1}{R}\frac{\partial v}{\partial x}\right)^2\right\} dxdy \end{aligned} \tag{17}$$

KINETIC ENERGY

The kinetic energy is the sum of the kinetic energies associated with axial, circumferential, and radial velocities, respectively; that is,

$$T = \frac{1}{2}\int_0^{\ell}\int_0^{2\pi R}\int_{-h/2}^{+h/2} \rho\left[\left(\frac{\partial u}{\partial t}\right)^2 + \left(\frac{\partial v}{\partial t}\right)^2 + \left(\frac{\partial w}{\partial t}\right)^2\right] dx\,dy\,dz \qquad (18)$$

Integration over the constant thickness yields

$$T = \frac{1}{2}\rho h\int_0^{\ell}\int_0^{2\pi R}\left[\left(\frac{\partial u}{\partial t}\right)^2 + \left(\frac{\partial v}{\partial t}\right)^2 + \left(\frac{\partial w}{\partial t}\right)^2\right] dx\,dy \qquad (19)$$

VARIATIONAL PRINCIPLE

The application of Hamilton's principle requires that the simultaneous first-order change in the Lagrangian $(L = T-U)$, integrated over a specified time interval, with respect to admissible variations in the degrees of freedom characterizing the state of strain (namely, u, v, and w) must vanish; that is,

$$\delta_{u,v,w}\int_{t_1}^{t_2} (T-U)\,dt = 0 \qquad (20)$$

Enforcement of this condition yields the Euler equations of the variation, or the differential equations of motion of the shell, together with the attendant boundary terms.

EULER EQUATIONS

The Euler equations (that is, the displacement equations of motion), valid for both periodic or nonperiodic motions, resulting from the variation are given by

$$\frac{E}{(1-\nu^2)}\left\{\frac{\partial}{\partial x}\left[\frac{\partial u}{\partial x} + \frac{1}{2}\left(\frac{\partial w}{\partial x}\right)^2\right] + \nu\frac{\partial}{\partial x}\left[\frac{\partial v}{\partial y} - \frac{w}{R} + \frac{1}{2}\left(\frac{\partial w}{\partial y}\right)^2 - \frac{v}{R}\frac{\partial w}{\partial y}\right]\right.$$
$$\left. + \frac{(1-\nu)}{2}\frac{\partial}{\partial y}\left[\frac{\partial u}{\partial y} + \frac{\partial v}{\partial x} + \frac{\partial w}{\partial x}\frac{\partial w}{\partial y} + \frac{v}{R}\frac{\partial w}{\partial x}\right]\right\} = \rho\frac{\partial^2 u}{\partial t^2} \qquad (21)$$

$$\frac{E}{(1-\nu^2)}\left\{\frac{\partial}{\partial y}\left[\frac{\partial v}{\partial y}-\frac{w}{R}+\frac{1}{2}\left(\frac{\partial w}{\partial y}\right)^2+\frac{v}{R}\frac{\partial w}{\partial y}\right]-\frac{1}{R}\frac{\partial w}{\partial y}\left[\frac{\partial v}{\partial y}-\frac{w}{R}+\frac{1}{2}\left(\frac{\partial w}{\partial y}\right)^2\right.\right.$$
$$\left.+\frac{v}{R}\frac{\partial w}{\partial y}\right]+\nu\frac{\partial}{\partial y}\left[\frac{\partial u}{\partial x}+\frac{1}{2}\left(\frac{\partial w}{\partial x}\right)^2\right]-\frac{\nu}{R}\frac{\partial w}{\partial y}\left[\frac{\partial u}{\partial x}+\frac{1}{2}\left(\frac{\partial w}{\partial x}\right)^2\right]$$
$$+\frac{(1-\nu)}{2}\frac{\partial}{\partial x}\left[\frac{\partial u}{\partial y}+\frac{\partial v}{\partial x}+\frac{\partial w}{\partial x}\frac{\partial w}{\partial y}+\frac{v}{R}\frac{\partial w}{\partial x}\right]-\frac{(1-\nu)}{2}\frac{1}{R}\frac{\partial w}{\partial x}\left[\frac{\partial u}{\partial y}+\frac{\partial v}{\partial x}\right.$$
$$\left.+\frac{\partial w}{\partial x}\frac{\partial w}{\partial y}+\frac{v}{R}\frac{\partial w}{\partial x}\right]+\frac{h^2}{12}\left(\frac{1}{R}\right)\frac{\partial}{\partial y}\left(\frac{\partial^2 w}{\partial y^2}+\frac{1}{R}\frac{\partial v}{\partial y}\right)+\frac{h^2}{12}\left(\frac{\nu}{R}\right)\frac{\partial}{\partial y}\left(\frac{\partial^2 w}{\partial x^2}\right)$$
$$\left.+\frac{h^2}{12}\frac{(1-\nu)}{2}\frac{1}{R}\frac{\partial}{\partial x}\left(2\frac{\partial^2 w}{\partial x\partial y}+\frac{1}{R}\frac{\partial v}{\partial x}\right)\right\}=\rho\frac{\partial^2 v}{\partial t^2} \qquad (22)$$

and

$$D\nabla^4 w+\frac{D}{R}\frac{\partial}{\partial y}(\nabla^2 v)-\frac{Eh}{(1-\nu^2)}\frac{\partial}{\partial x}\left\{\frac{\partial w}{\partial x}\left[\frac{\partial u}{\partial x}+\frac{1}{2}\left(\frac{\partial w}{\partial x}\right)^2\right]\right\}$$
$$-\frac{Eh}{(1-\nu^2)}\frac{\partial}{\partial x}\left\{\nu\frac{\partial w}{\partial x}\left[\frac{\partial v}{\partial y}-\frac{w}{R}+\frac{1}{2}\left(\frac{\partial w}{\partial y}\right)^2+\frac{v}{R}\left(\frac{\partial w}{\partial y}\right)\right]\right\}$$
$$-\frac{Eh}{(1-\nu^2)}\frac{\partial}{\partial y}\left\{\frac{\partial w}{\partial y}\left[\frac{\partial v}{\partial y}-\frac{w}{R}+\frac{1}{2}\left(\frac{\partial w}{\partial y}\right)^2+\frac{v}{R}\frac{\partial w}{\partial y}\right]\right\}$$
$$-\frac{Eh}{(1-\nu^2)}\frac{\partial}{\partial y}\left\{\nu\frac{\partial w}{\partial y}\left[\frac{\partial u}{\partial x}+\frac{1}{2}\left(\frac{\partial w}{\partial x}\right)^2\right]\right\}-\frac{Eh}{(1-\nu^2)}\frac{1}{R}\left\{\frac{\partial v}{\partial y}-\frac{w}{R}\right.$$
$$+\frac{1}{2}\left(\frac{\partial w}{\partial y}\right)^2+\frac{v}{R}\frac{\partial w}{\partial y}-\nu\left[\frac{\partial u}{\partial x}+\frac{1}{2}\left(\frac{\partial w}{\partial x}\right)^2\right]\Bigg\}-\frac{Eh}{(1-\nu^2)}\frac{\partial}{\partial y}\left\{\frac{v}{R}\left[\frac{\partial v}{\partial y}\right.\right.$$
$$\left.\left.-\frac{w}{R}+\frac{1}{2}\left(\frac{\partial w}{\partial y}\right)^2+\frac{v}{R}\left(\frac{\partial w}{\partial y}\right)\right]+\nu\frac{v}{R}\left[\frac{\partial u}{\partial x}+\frac{1}{2}\left(\frac{\partial w}{\partial x}\right)^2\right]\right\}$$

(Continued)

$$+\frac{Eh}{2(1+\nu)}\frac{\partial}{\partial y}\left\{\frac{\partial w}{\partial x}\left[\frac{\partial u}{\partial y}+\frac{\partial v}{\partial x}+\frac{\partial w}{\partial x}\frac{\partial w}{\partial y}+\frac{v}{R}\frac{\partial w}{\partial x}\right]\right\}$$

$$+\frac{Eh}{2(1+\nu)}\frac{\partial}{\partial x}\left\{\left(\frac{\partial w}{\partial y}+\frac{v}{R}\right)\left[\frac{\partial u}{\partial y}+\frac{\partial v}{\partial x}+\frac{\partial w}{\partial x}\frac{\partial w}{\partial y}+\frac{v}{R}\frac{\partial w}{\partial x}\right]\right\} = -\rho h\frac{\partial^2 w}{\partial t^2} \tag{23}$$

The foregoing displacement equations of motion can be written in a more concise form by employing Hooke's law. Since Hooke's law states that

$$\left.\begin{aligned}\sigma_x^0 &= \frac{E}{(1-\nu^2)}\left[\epsilon_x^0+\nu\,\epsilon_y^0\right]\\ \sigma_y^0 &= \frac{E}{(1-\nu^2)}\left[\epsilon_y^0+\nu\,\epsilon_x^0\right]\\ \tau_{xy}^0 &= \frac{E}{2(1+\nu)}\gamma_{xy}^0\end{aligned}\right\} \tag{24}$$

then, though utilization of Equation (24), the equations of motion can be written as

$$\frac{\partial\sigma_x^0}{\partial x}+\frac{\partial\tau_{xy}^0}{\partial y} = \rho\frac{\partial^2 u}{\partial t^2} \tag{25}$$

$$\frac{\partial\sigma_y^0}{\partial y}+\frac{\partial\tau_{xy}^0}{\partial x}-\frac{1}{R}\left[\sigma_y^0\frac{\partial w}{\partial y}+\tau_{xy}^0\frac{\partial w}{\partial x}\right]+\frac{E}{(1-\nu^2)}\frac{h^2}{12}\left(\frac{1}{R}\right)\left\{\frac{\partial^3 w}{\partial y^3}+\frac{\partial^3 w}{\partial x^2\partial y}\right.$$

$$\left.+\frac{1}{R}\left[\frac{(1-\nu)}{2}\frac{\partial^2 v}{\partial x^2}+\frac{\partial^2 v}{\partial y^2}\right]\right\} = \rho\frac{\partial^2 v}{\partial t^2} \tag{26}$$

and

$$D\nabla^4 w+\frac{D}{R}\frac{\partial}{\partial y}(\nabla^2 v)-h\frac{\partial}{\partial x}\left[\sigma_x^0\frac{\partial w}{\partial x}+\tau_{xy}^0\left(\frac{\partial w}{\partial y}+\frac{v}{R}\right)\right]$$

$$-h\frac{\partial}{\partial y}\left[\sigma_y^0\frac{\partial w}{\partial y}+\tau_{xy}^0\frac{\partial w}{\partial x}\right]-\sigma_y\left(\frac{h}{R}\right) = -\rho h\frac{\partial^2 w}{\partial t^2} \tag{27}$$

The equations can be written in a still more compact form by the introduction of shear and bending moment resultants defined as follows (see Figure 2):

$$\left.\begin{aligned} M_x &\equiv \int_{-h/2}^{+h/2} z\,\sigma_x\,dz \\ M_y &\equiv \int_{-h/2}^{+h/2} z\,\sigma_y\,dz \\ M_{xy} &\equiv \int_{-h/2}^{+h/2} z\,\tau_{xy}\,dz \\ Q_x &\equiv \frac{\partial M_x}{\partial x} + \frac{\partial M_{xy}}{\partial y} \\ Q_y &\equiv \frac{\partial M_y}{\partial y} + \frac{\partial M_{xy}}{\partial x} \end{aligned}\right\} \qquad (28)$$

Then use of the definitions given by Equation (28) allows the equations of motion to be written as

$$\frac{\partial \sigma_x^0}{\partial x} + \frac{\partial \tau_{xy}^0}{\partial y} = \rho \frac{\partial^2 u}{\partial t^2} \qquad (29)$$

$$\frac{\partial \sigma_y^0}{\partial y} + \frac{\partial \tau_{xy}^0}{\partial x} - \frac{1}{R}\left[\sigma_y^0 \frac{\partial w}{\partial y} + \tau_{xy}^0 \frac{\partial w}{\partial x}\right] - \left(\frac{1}{Rh}\right) Q_y = \rho \frac{\partial^2 v}{\partial t^2} \qquad (30)$$

and

$$\frac{\partial^2 M_x}{\partial x^2} + 2\frac{\partial^2 M_{xy}}{\partial x \partial y} + \frac{\partial^2 M_y}{\partial y^2} + h\frac{\partial}{\partial x}\left[\sigma_x^0 \frac{\partial w}{\partial x} + \tau_{xy}^0\left(\frac{\partial w}{\partial y} + \frac{v}{R}\right)\right] + h\frac{\partial}{\partial y}\left[\sigma_y^0 \frac{\partial w}{\partial y} + \tau_{xy}^0 \frac{\partial w}{\partial x}\right] + \left(\frac{h}{R}\right)\sigma_y = -\rho h \frac{\partial^2 w}{\partial t^2} \qquad (31)$$

or in the linearized form as

$$\frac{\partial \sigma_x^0}{\partial x} + \frac{\partial \tau_{xy}^0}{\partial y} = \rho \frac{\partial^2 u}{\partial t^2} \tag{32}$$

$$\frac{\partial \sigma_y^0}{\partial y} + \frac{\partial \tau_{xy}^0}{\partial x} - \left(\frac{1}{Rh}\right) q_y = \rho \frac{\partial^2 v}{\partial t^2} \tag{33}$$

and

$$\frac{\partial^2 M_x}{\partial x^2} + 2 \frac{\partial^2 M_{xy}}{\partial x \partial y} + \frac{\partial^2 M_y}{\partial y^2} + \left(\frac{h}{R}\right) \sigma_y = - \rho h \frac{\partial^2 w}{\partial t^2} \tag{34}$$

The linearized equations of motion, reduced to the static case, are not identical to the linear set presented by Sanders in Reference 20. The only difference between the two sets of linear equations is a consequence of the neglect, in the present development, of effects associated with rotations about the normal to the shell midsurface.

BOUNDARY CONDITIONS

The boundary conditions which result from application of Hamilton's principle (Equation (20)) are given, for both periodic and nonperiodic motions, in general form as

$$h\sigma_x^0 = 0 \quad \text{or} \quad \delta u = 0 \quad \text{at} \quad x = 0, \ell \tag{35}$$

$$h\tau_{xy}^0 + \frac{D}{R} \frac{(1-\nu)}{2} 2 \left(\frac{\partial^2 w}{\partial x \partial y} + \frac{1}{R} \frac{\partial v}{\partial x} \right) = 0 \quad \text{or} \quad \delta v = 0 \quad \text{at} \quad x = 0, \ell \tag{36}$$

$$\left\{ - D \left[\frac{\partial^3 w}{\partial x^3} + (2-\nu) \frac{\partial^3 w}{\partial x \partial y^2} + \frac{1}{R} \frac{\partial^2 v}{\partial x \partial y} \right] + h\sigma_x^0 \left(\frac{\partial w}{\partial x} \right) + h\tau_{xy}^0 \left(\frac{\partial w}{\partial y} + \frac{v}{R} \right) \right\} = 0 \quad \text{or} \quad \delta w = 0 \quad \text{at} \quad x = 0, \ell \tag{37}$$

and

$$\left[D\left(\frac{\partial^2 w}{\partial x^2}\right) + \nu\left(\frac{\partial^2 w}{\partial y^2} + \frac{1}{R}\frac{\partial v}{\partial y}\right)\right] = 0 \quad \text{or} \quad \delta\left(\frac{\partial w}{\partial x}\right) = 0 \quad \text{at} \quad x = 0, \ell \tag{38}$$

REDUCTION TO CLASSICAL EQUATIONS

A simplified set of Euler equations can be obtained if the Karman-Donnell strain-displacement relations are used in place of the more complicated set of strain-displacement relations given by Equations (13), (14), and (15). The Karman-Donnell strain-displacement relations are given by

$$\epsilon_x = \frac{\partial u}{\partial x} + \frac{1}{2}\left(\frac{\partial w}{\partial x}\right)^2 - z\frac{\partial^2 w}{\partial x^2} \tag{39}$$

$$\epsilon_y = \frac{\partial v}{\partial y} - \frac{w}{R} + \frac{1}{2}\left(\frac{\partial w}{\partial y}\right)^2 - z\frac{\partial^2 w}{\partial y^2} \tag{40}$$

$$\gamma_{xy} = \frac{\partial u}{\partial y} + \frac{\partial v}{\partial x} + \frac{\partial w}{\partial x}\frac{\partial w}{\partial y} - 2z\frac{\partial^2 w}{\partial x \partial y} \tag{41}$$

Substituting Equations (39), (40), and (41) into the Lagrangian and carrying out the variations in accordance with Hamilton's principle leads to the following simplified set of stress-displacement equations of motion for the axial, circumferential, and radial directions, respectively.

$$\frac{\partial \sigma_x^0}{\partial x} + \frac{\partial \tau_{xy}^0}{\partial y} = \rho\frac{\partial^2 u}{\partial t^2} \tag{42}$$

$$\frac{\partial \sigma_y^0}{\partial y} + \frac{\partial \tau_{xy}^0}{\partial x} = \rho\frac{\partial^2 v}{\partial t^2} \tag{43}$$

and

$$D\nabla^4 w - h\frac{\partial}{\partial x}\left[\sigma_x^0\frac{\partial w}{\partial x} + \tau_{xy}^0\frac{\partial w}{\partial y}\right] - h\frac{\partial}{\partial y}\left[\sigma_y^0\frac{\partial w}{\partial y} + \tau_{xy}^0\frac{\partial w}{\partial x}\right] - \sigma_y\left(\frac{h}{R}\right) = -\rho h\frac{\partial^2 w}{\partial t^2} \tag{44}$$

Now, if the motion is predominantly radial (as when there are a large number of circumferential waves in the modal pattern), then Equations (42), (43), and (44) admit still another and quite drastic simplification, that of neglecting the midsurface inertia terms. The justification for this simplification was first noted by Reissner.[6] Thus, with the midsurface inertia terms omitted, the equilibrium equations become

$$\frac{\partial\sigma_x^0}{\partial x} + \frac{\partial\tau_{xy}^0}{\partial y} = 0 \tag{45}$$

$$\frac{\partial\sigma_y^0}{\partial y} + \frac{\partial\tau_{xy}^0}{\partial x} = 0 \tag{46}$$

and

$$D\nabla^4 w - h\frac{\partial}{\partial x}\left[\sigma_x^0\frac{\partial w}{\partial x} + \tau_{xy}^0\frac{\partial w}{\partial y}\right] - h\frac{\partial}{\partial y}\left[\sigma_y^0\frac{\partial w}{\partial y} + \tau_{xy}^0\frac{\partial w}{\partial x}\right] - \sigma_y\left(\frac{h}{R}\right) = -\rho h\frac{\partial^2 w}{\partial t^2} \tag{47}$$

Equations (45) and (46) can now be satisfied identically by the introduction of an Airy stress function F defined such that

$$\left.\begin{aligned}\sigma_x^0 &= \frac{\partial^2 F}{\partial y^2}\\ \sigma_y^0 &= \frac{\partial^2 F}{\partial x^2}\\ \tau_{xy}^0 &= -\frac{\partial^2 F}{\partial x\partial y}\end{aligned}\right\} \tag{48}$$

Then, use of Equations (45), (46), and (48) permits the lateral equilibrium equation to be written as

$$D\nabla^4 w - h\left[\frac{\partial^2 F}{\partial y^2}\frac{\partial^2 w}{\partial x^2} - 2\frac{\partial^2 F}{\partial x \partial y}\frac{\partial^2 w}{\partial x \partial y} + \frac{\partial^2 F}{\partial x^2}\frac{\partial^2 w}{\partial y^2}\right] - \left(\frac{h}{R}\right)\frac{\partial^2 F}{\partial x^2} = -\rho h \frac{\partial^2 w}{\partial t^2} \qquad (49)$$

A second equation involving the stress function and the radial displacement can be obtained by combining Equations (24), (39), (40), (41), (45), (46), and (48) to yield

$$\nabla^4 F = E\left[\left(\frac{\partial^2 w}{\partial x \partial y}\right)^2 - \frac{\partial^2 w}{\partial x^2}\frac{\partial^2 w}{\partial y^2}\right] - \frac{E}{R}\frac{\partial^2 w}{\partial x^2} \qquad (50)$$

This compatibility equation was developed first by Donnell.[7] Equations (49) and (50), with the radial inertia term omitted, are one of the equation sets commonly referred to as the Karman-Donnell equations; these equations govern the large-deflection behavior of thin shells in the presence of midsurface forces.

METHOD OF SOLUTION

The differential equations obtained in the previous section which reflect the utilization of strain-displacement relations equivalent to those of Sanders are three highly nonlinear coupled equations in the three dependent variables u, v, and w. On the other hand, Karman-Donnell strain-displacement relations, with the midsurface inertia terms neglected, admit the reduction to two simultaneous differential equations involving only the stress function and the radial displacement. This reduced set of two simultaneous equations is still highly nonlinear and coupled but is much more manageable than the set of three simultaneous differential equations. The solutions reflecting the use of both sets of strain-displacement relations are obtained by employing the direct method of the calculus of variations (that is, the Rayleigh-Ritz method). The solutions corresponding to the strain-displacement relations which result in the Karman-Donnell equations ((49) and (50)) are discussed first for the case when a large number of circumferential waves are present. The solutions corresponding to the Sanders strain-displacement relations (Equations (21), (22), and (23)) are discussed subsequently for the case when a small number of circumferential waves occurs.

SOLUTIONS FOR A LARGE NUMBER OF CIRCUMFERENTIAL WAVES

In all of the existing analytical studies of the nonlinear vibrations of thin, circular cylindrical shells, except for the work reported in References 13 and 16, it is assumed that (1) the radial displacement is representable by a chessboard pattern, (2) the shell possesses many circumferential waves (that is, the shallow-shell behavior), and (3) the midsurface inertia terms can be neglected. If indeed there are a large number of circumferential waves present, then assumption (3) seems intuitively correct. Assumption (1), however, seems intuitively incorrect. As noted by References 13 and 16, utilization of the chessboard pattern for the radial displacement leads to a violation of the periodicity condition for the circumferential displacement. Even if the periodicity condition relative to a chessboard pattern for the radial displacement

could be satisfied by selecting a special homogeneous solution for the stress function (Reference 13 alludes to having accomplished this, but no details are presented), it still seems intuitively incorrect that the radial displacement pattern for a large number of circumferential waves would be an exact chessboard pattern. Some consideration must be given to the degree of midsurface stretching and, consequently, to the increased level of energy that would be necessary to produce a pure chessboard pattern. It would appear that, for finite radial displacements, a displacement pattern which allows the shell to move inward would be more likely to occur since this type of displacement pattern should involve less energy and, hence, lead to the equilibrium position that the shell would seek. This intuitive reasoning, which is founded on a knowledge of shell behavior in the axial compression postbuckling problem, is shown in retrospect to be justified.

Fixed Parameter Solution (n Large)

For a uniform homogeneous shell, the study reported in Reference 16 is based on the assumption that the radial displacement which satisfies the geometrical constraints of the problem (that is, freely supported ends) is representable, save for a shift of coordinate system origin, in the following form:

$$\left(\frac{w}{h}\right) = y_1(t) \cos\frac{\pi x}{\lambda_x} \cos\frac{\pi y}{\lambda_y} + \frac{\eta}{8} y_1^2(t) \cos\frac{2\pi x}{\lambda_x} + \frac{\eta}{8} y_1^2(t) \qquad (51)$$

where $y_1(t)$ is an arbitrary function of time. The above choice of deflected shape, while not being perfectly general, is a discerning one in that, in addition to satisfying the geometric boundary conditions, it also leads to satisfaction of the continuity constraint on the circumferential displacement. Further, by restricting the time dependent coefficients to terms proportional to $y_1(t)$ and $y_1^2(t)$, the resultant motion is forced to be periodic, although not harmonic.

In Reference 16, the Galerkin procedure was used to obtain the governing differential equations; subsequent solution of the equations was carried out by means of a perturbation technique. Since the Galerkin integral-

approach discloses no information relative to energy level, the present investigation reformulates and solves the problem by using the variational approach: the radial displacement given by Equation (51), together with the stresses obtained from Equations (48) and (50), is substituted into the Lagrangian (see Appendix I for development). The enforcement of the vanishing of the first variation of the Lagrangian with respect to $y_1(\tau)$ leads to a single second-order nonlinear differential equation with $y_1(\tau)$ as the dependent variable. After reduction of the single second-order differential equation to two coupled first-order differential equations, the solution is obtained by employing a standard Kutta-Merson numerical method.

The results obtained verify that the curves in Reference 16 representing the nonlinear free, but periodic, vibrational characteristics are indeed correct. These results are shown in Figures 3 and 4.

However, the occurrence of the multivalued conditions of (1) different amplitudes for a given wave pattern at a fixed value of the frequency and (2) different wave patterns for the same amplitude at a given frequency requires the approach of the present analysis, which establishes the lowest level of energy associated with a particular condition. The discussion of this point is expanded in the section on "Results and Discussion". It is also observed that the periodic solution, which is based upon a vanishing radial deflection at the cylinder ends, implies that the vibrational behavior is influenced by the boundary conditions in the presence of a modal pattern containing a small number of axial waves. Although the case of a small number of axial waves is not the general problem being investigated herein, it will be shown in the next section that a more general radial deflection function (one which results in the vanishing of the radial deflection at the shell ends and leads to satisfaction of the v-displacement periodicity condition) does not reflect necessarily a periodic motion based upon the minimum energy criterion. For long shells (large number of axial waves), the nonperiodic vibrational behavior is shown, for all cases, to correspond to the minimum energy solution when the parameters of the radial deflection function of Reference 16 are free rather than fixed.

Free Parameter Solution (n Large)

If the shell modal pattern reflects several or more waves in the axial direction, then it is reasonable to assume that the boundary conditions will not significantly influence the frequency of vibration. Then the deflected shape used in the fixed parameter solution of the previous section can be made more general and representable as

$$\left(\frac{w}{h}\right) = y_1(t) \cos\frac{\pi x}{\lambda_x} \cos\frac{\pi y}{\lambda_y} + y_3(t) \cos\frac{2\pi x}{\lambda_x} + y_5(t) \tag{52}$$

where $y_1(t)$, $y_3(t)$, and $y_5(t)$ are arbitrary functions of time. The substitution of the radial displacement given by Equation (52) and its associated stress function, obtained from Equation (50), into the continuity condition for the circumferential displacement yields the requirement

$$y_5(t) = \frac{\eta}{8} y_1^2(t) \tag{53}$$

Hence, the deflected shape is now given by

$$\left(\frac{w}{h}\right) = y_1(t) \cos\frac{\pi x}{\lambda_x} \cos\frac{\pi y}{\lambda_y} + y_3(t) \cos\frac{2\pi x}{\lambda_x} + \frac{\eta}{8} y_1^2(t) \tag{54}$$

The substitution of the radial displacement given by Equation (54), together with the stresses obtained from Equations (48) and (50), into the Lagrangian (see Appendix I for development), and enforcement of the vanishing of the first variation of the Lagrangian with respect to $y_1(\tau)$ and $y_3(\tau)$ lead to two second-order nonlinear differential equations with $y_1(\tau)$ and $y_3(\tau)$ as the independent variables. After a change of the independent variable and subsequent reduction of the two second-order differential equations to four first-order differential equations, the solution is obtained by employing a standard Kutta-Merson numerical method.

A comparison of the maximum radial displacement for the fixed parameter solution possessing the same modal shape and the same initial conditions is shown on Figure 5. The free parameter solution, reflecting only a

change in the initial value of y_3 , leading to the minimum energy solution is shown in Figure 6.

A comparison of the nondimensional strain energy parameter for the cases where the initial velocities are zero is given in Figures 7, 8, and 9 for different combinations of the modal shape and initial displacements.

When the shell modal pattern reflects a small number of axial waves, the choice of deflected shape, which enforces the vanishing radial deflection condition at the shell ends, can be made more general than that given in Reference 16 and is representable as

$$\left(\frac{w}{h}\right) = y_1(t) \cos\frac{\pi x}{\lambda_x} \cos\frac{\pi y}{\lambda_y} - \left[y_3(t) + \frac{\eta}{8} y_1^2(t)\right] \cos\frac{4\pi x}{\lambda_x}$$

$$- y_3(t) \cos\frac{2\pi x}{\lambda_x} + \frac{\eta}{8} y_1^2(t) \qquad (55)$$

The radial deflection (Equation (55)) leads to identical satisfaction of the v-displacement periodicity condition. The resulting solution, obtained in a manner analogous to the previous free parameter solution, yields a nonperiodic vibrational behavior. A comparison of the maximum radial displacements, reflecting the different assumed deflection functions, is given on Figure 5.

SOLUTION FOR A SMALL NUMBER OF CIRCUMFERENTIAL WAVES

For a uniform homogeneous shell, the strain energy and the kinetic energy are given by Equations (17) and (18), respectively. Functions representing the degrees of freedom u , v , and w , which satisfy the continuity condition on the circumferential displacement but are arbitrary with time, may be taken in the form

$$\left(\frac{w}{h}\right) = y_1(t) \cos\frac{\pi x}{\lambda_x} \cos\frac{\pi y}{\lambda_y}$$

$$n\left(\frac{u}{h}\right) = y_3(t) \sin\frac{\pi x}{\lambda_x} \cos\frac{\pi y}{\lambda_y} + y_5(t) \sin\frac{2\pi x}{\lambda_x} \cos\frac{2\pi y}{\lambda_y} + y_7(t) \sin\frac{3\pi x}{\lambda_x} \Bigg\} \qquad (56)$$

(Continued)

$$n\left(\frac{v}{h}\right) = \cdot\, y_9(t)\cos\frac{\pi x}{\lambda_x}\sin\frac{\pi y}{\lambda_y} + y_{11}(t)\cos\frac{2\pi x}{\lambda_x}\sin\frac{2\pi y}{\lambda_y} + y_{13}(t)\sin\frac{2\pi y}{\lambda_y}\Bigg)$$

where $y_1(t)$, $y_3(t)$, $y_5(t)$, $y_7(t)$, $y_9(t)$, $y_{11}(t)$, and $y_{13}(t)$ are arbitrary functions of time. Now, the substitution of Equation (56) into Equations (17) and (18) and the enforcement of the simultaneous vanishing of the first variation of the Lagrangian (L = T-U) with respect to $y_1(\tau)$, $y_3(\tau)$, $y_5(\tau)$, $y_7(\tau)$, $y_9(\tau)$, $y_{11}(\tau)$, and $y_{13}(\tau)$ lead to a set of seven second-order nonlinear coupled differential equations. After a change of the independent variable and subsequent reduction of the 7 second-order differential equations to 14 first-order differential equations (the details of which are given in Appendix III), the solution is obtained by employing a standard Kutta-Merson numerical method.

The degree and character of the nonlinearity, reflecting the employment of the modified Sanders strain-displacement relations, are shown in Figures 10 and 11 for the case of finite initial displacements but zero initial velocities.

RESULTS AND DISCUSSION

In the free vibration of a physical system represented or idealized by a set of linearized equations, the magnitude of the resulting displacements and the energy associated with these displacements is indeterminate. However, if the equations representing the physical system are not linearized, the displacements and the attendant energy then possess a unique determinate value for any given set of initial conditions.

It is known that in the solution of the postbuckling problem of a thin, circular cylindrical shell, the determination of the minimum energy is of primary importance. One of the solutions given in Reference 12 predicts that the shell will be in tension in the postbuckled state under the action of an applied compressive end load. This predicted solution is obviously incorrect, as is pointed out in Reference 21. The solution is rejected because it does not, in general, represent the minimum energy for the particular choice of radial deflection function selected. Hence, since energy considerations are important in the understanding and comprehension of the nonlinear shell postbuckling problem, it would appear that these same considerations would prove to be vitally important to any solutions of the nonlinear shell vibration problem.

That the energy level for a given modal shape might be an important consideration has not been brought out or explored to date. The most advanced solution of the nonlinear shell vibration problem (Reference 16) makes no mention of energy considerations relative to the assumed modal shape. It is stated in Reference 14 that, for a large number of circumferential waves, the square wave pattern (that is, the chessboard pattern) has the least strain energy. However, this statement is not correct, and this point is discussed later in this section.

Still another important facet in the understanding of the nonlinear free vibration problem of a thin, circular shell involves an analogy to the static instability problem. In the nonlinear shell postbuckling problem (see, for example, Reference 22), the simultaneous minimization is made with respect to the free parameters in the assumed deflected shape and also with respect to the modal wave parameters μ and η. As such, the number of axial and circumferential waves is continuously varying as the minimization is accomplished. However, the shell instability problem is treated by means of a static analysis, and a slightly different approach is necessary in the free vibration problem. In the linear and nonlinear free vibration problem, the basic assumption is introduced that the wave parameters μ and η are not variables but are constant. This assumption essentially implies that, if an experiment were being conducted, and if the modal shape and modal lines ($w = 0$) could be detected, then this modal shape and its modal lines would not vary with time. The implication of this assumption relative to the assumed modal shapes chosen in the previous section is discussed subsequently.

The deflected shape chosen in Reference 16 (that is, the fixed parameter solution reflecting a large number of circumferential waves) is a judicious choice. It has been shown in References 4, 5, 9, 10, and 11 that the chessboard pattern is indeed the pattern which the shell seeks when the displacements involved are infinitesimal. Hence, it would seem logical to assume that a slightly modified chessboard pattern might emerge as the modal pattern when the displacements are increased from infinitesimal to finite values. In the analogous shell buckling problem (see, for example References 12 or 22), three of the most important terms in the representation of the radial deflection are those selected in Reference 16. In addition, the deflected shape selected in Reference 16 reflects zero radial displacement at the ends of the shell and leads to a periodic solution in time when the continuity condition on the v-displacement is enforced.

Figures 3 and 4 depict the frequency behavior for the resultant periodic motion as a function of the amplitude. The nonlinearity of the resulting motion and the degree of hardness or softness of the system are highly dependent upon the value of the wave parameter η ; for the same initial displacement (assuming an initial velocity of zero), the nonlinearity becomes more pronounced as the value of η increases. Hence, for a particular shell geometry (fixed (h/R)) and a fixed set of initial conditions, the degree of nonlinearity is increased as the number of circumferential waves becomes larger.

It can be further noted from Figures 3 and 4 that the character of the nonlinearity is dependent upon the value of the full wave aspect ratio μ . In general, the results show that the vibrations usually exhibit a softening character when $\mu < 1$ and a hardening character when $\mu > 1$. In the present analysis, the strain energies associated with the various choices of initial conditions and wave parameters have been determined. Several values of the energy appear on Figures 3 and 4. In particular, it is noted that at a certain set of fixed initial conditions (an initial displacement of unity and an initial velocity of zero) the energy increases considerably as the value of the full wave aspect ratio μ increases (see Figure 4). This is more clearly shown in Figure 12. In a like manner, the increase in energy associated with an increase in the wave parameter η is shown on Figure 13.

It is noted that at the crossover points on Figure 3, the energies are not the same. For instance, at the point corresponding to the coordinates $y_1 = 1.91$ and $\omega_{K-D}/\omega_L = 0.75$, the energy associated with the $\mu = 1$ modal shape is 185% higher than the energy associated with the $\mu = 0.707$ modal shape. This indicates that for the same frequency and displacement, the modal shape is dependent upon the energy. Hence, in an experiment where a large frequency spectrum is examined, certain modes may never appear if the vibration excitor cannot inject sufficient energy to the shell. This is particularly true for the higher levels of energy which occur for $\mu > 1$.

Another point not mentioned in Reference 16, but worthy of mention here, can be noted in Figure 14, which is a partial plot of the modal shape for the listed choice of deflected shape. As can be seen in Figure 14, the aspect ratio is not constant but is variable. However, if the whole wavelength of modal shape is considered and the aspect ratio of the waveform is taken as the average over this whole wavelength, then it can be considered as a constant.

Further, it should be pointed out that the solution obtained in Reference 16 is presumably valid for the range of values of the wave parameters presented. As such, the solution should be valid when the number of axial waves is large or small. However, it appears that while the solution presented in Reference 16 is the most advanced solution to date, new insight into the problem is gained through energy considerations. The result of freeing all parameters in the assumed radial deflection functions, compatible with assuring the continuity condition on the v-displacement, leads to nonperiodic motions when the number of axial waves is either large or small. Also, although the motion is nonperiodic, strictly speaking, in certain cases it appears similar to the periodic fixed-parameter solution (see Figures 5 and 6). Hence, too casual an observation of experimental results might lead to the erroneous conclusion that the motion is periodic.

When the number of axial waves is small, the energy levels reflecting the deflected shapes (Equations (51) or (55)) are identical for the present choice of initial conditions, but the more general choice of deflected shape (Equation (55)) leads to a nonperiodic motion while the solution of Reference 16 (that is, Equation (51)) leads to a periodic motion (see Figure 5). Although the case of a small number of axial waves is not the case of interest for the present investigation, it is highly probable that introducing a still more general radial deflection function for the "freely supported" case will yield a nonperiodic solution which possesses a lower energy level than that associated with the radial deflection functions given by Equations (51) and (55). This conjecture is based on the known tendency for thin cylinders deformed into many waves to depart more and

more from the chessboard modal pattern as larger and larger amplitudes of the radial deflection occur.

When the number of axial waves is large, the nonperiodic solution, which reflects the radial deflection given by Equation (54), leads to a lower energy than the periodic solution (Equation (51)). The lower energy, associated with the nonperiodic solution, can be seen on Figures 7, 8, and 9. On Figure 7, the minimum energy occurs almost identically at the value of y_3 which Reference 16 employs. That is, however, only chance occurrence. In Figure 8, the true minimum energy solution reflects a significant difference in the value of y_3 from that which was utilized in Reference 16. Further, it is interesting to note that a lower value of the y_1 displacement shifts the y_3 value for the minimum energy from a higher to a lower value. From this observation and a perusal of the strain energy expression for the free parameter solution (see Equation (68)), an important physical consequence can be deduced. As the value of y_1 becomes smaller and smaller (that is, as it approaches infinitesimal values), the minimum point shifts farther and farther to the left; this leads to the conclusion that for infinitesimal values of y_1 , the minimum energy is the solution corresponding to $y_3 = 0$. This observation, coupled with the fact that $y_1 < 1$ implies that $y_1^2 \ll 1$, leads to the conclusion that in approaching the limit of infinitesimal displacements, the least energy solution reflects the chessboard pattern. That this is true can also be deduced from Figure 9. This figure shows that for a small value of displacement $(y_1 = 0.01)$, the minimum energy solution exists for $y_3 = 0$; hence, further credence is given to the deduction discussed above. This deduction is important. It shows that only when the displacements are very small is the minimum energy solution representable as a chessboard pattern; it also shows that for finite displacements of the order of magnitude of the shell thickness, the minimum energy is related to a slightly modified chessboard pattern. This shows why in the linear, small displacement experimental studies (References 4, 5, 9, 10, and 11), the predominant evidence indicated that the chessboard pattern was the actual pattern developed by the vibrating shell.

Still another and important consideration deals with the validity of the solution concerning the rotation limits allowable within the scope of Karman-Donnell theory. This consideration was used in Reference 19 in discussing limitations on the validity of several well-known solutions of the postbuckled shell problem. The maximum rotations must be small in comparison to unity (5 percent is considered herein to be the limiting value). Then, Figures 15, 16, 17, and 18 show conservative estimates of the limitations inherent in the solution. The severe limitations on the $\mu = 2$ case (Figure 18) should be noted. For a $y_1 = 4$, the R/h of the shell must be greater than or equal to 4500 to be within the range of allowable rotations. Thus, for shells which are in the range of practical interest $(100 < \frac{R}{h} < 3000)$, the validity of the present solution would have to be restricted (for the $\mu = 2$ case) to smaller amplitudes. It may be noted further that the restrictions on the validity of the solutions are less stringent for other values of μ (see Figures 15, 16, and 17). Hence, unless the displacements experienced by the shell are relatively large, the limitations concerning the allowable rotation do not appear to be critical for the free vibration problem. However, these limitations could become considerably more important, for example, in a dynamic buckling or a forced vibration study.

For vibration with low values of n, the Sanders strain-displacement relations have been used and the midsurface inertia terms retained. With the retention of the midsurface inertia terms, the occurrence of three frequencies for each given modal configuration is possible (see, for example, References 4 and 5). However, each of the frequencies will have different amplitude ratios; of the three possible values of the frequency, the important one is that associated with the primarily radial motion of the shell walls. This value is several orders of magnitude lower than either of the other two, which are associated primarily with axial and circumferential motions, respectively. The deflected shapes and the attendant initial conditions assumed in this investigation again reflect the interest in only the motion which is predominantly radial.

Due to the complexity of this nonlinear shell vibration problem, the free vibration solutions presented herein are based only upon the basic chessboard modal pattern. For small amplitudes, the chessboard pattern continues to provide a periodic motion, which is not necessarily the true situation. Thus, where quantitative rather than qualitative behavior is of prime importance, the chessboard pattern must be modified to permit the possibility of the occurrence of a nonperiodic vibration behavior.

In the modal pattern associated with $n = 2$, the nonlinearity of the resultant motion, as in the case when the number of circumferential waves is large, is highly dependent upon the value of the wave parameter η. For a fixed number of circumferential waves (here $n = 2$), the low values of η reflect the behavior of a thin shell, whereas the larger values of η reflect the behavior of a thicker shell. Representative curves depicting this behavior are shown in Figures 10 and 11. In Figures 10 and 11, it is shown that no detectable nonlinearity is observed until the (R/h) ratio is less than 1000. For gradually increasing thickness, the nonlinearity becomes pronounced. In Figure 10 for a full wave aspect ratio of unity, the ratio of nonlinear to linear frequency for $(h/R) = 1/100$ and $(w/h) = 16$ reaches 1.165 or 16.5% beyond that which linear theory would predict. In Figure 11 for a full wave aspect ratio of 1/2, the ratio of nonlinear to linear frequency, again for $(h/R) = 1/100$ and $(w/h) = 16$, reaches 1.25 or 25% over that which linear theory predicts.

For the large values of deflection necessary to produce a pronounced nonlinearity when the number of circumferential waves is low, it is imperative to ascertain at what point the limitations on the rotations are exceeded. Representative values for $\eta = 0.04$ and $\mu = 1.0$ are shown on Figures 19 and 20. While these limitations are intended to be only a qualitative, conservative estimate, it is apparent that the $(\varphi_x)^2$ limitation is more critical than the $(\varphi_y)^2$ limitation. In particular, for $\eta = 0.04$ and $\mu = 1.0$, the data of Figure 20 predict that $(\varphi_x)^2$ will exceed its allowable limit for an $(R/h) = 100$ somewhere between the point where the initial y_1 displacement is between

10 and 12. For $y_1 = 12$, the character of the nonlinearity is given in Figure 10. Again, the consideration of the size-of-rotations limitation on the validity of the theory does not appear to be critical for the free vibration problem. However, large amplitude behavior, in connection with dynamic buckling or forced vibration analyses, could lead to restrictions on the validity of solutions for specific shell geometries.

CONCLUDING REMARKS

The governing differential equations and the attendant boundary conditions for the nonlinear free vibration of thin, circular cylindrical shells have been developed by variational procedures by the use of both the Karman-Donnell and a set of appropriately modified Sanders strain-displacement relations. Approximate solutions, obtained by the direct variational approach, are utilized to re-examine and provide new interpretation to established approximate solutions for shells possessing a large number of circumferential waves (that is, when the Karman-Donnell formulation is valid). Approximate solutions, which reflect the use of the modified Sanders formulation for shells possessing a small number of circumferential waves, are obtained and are believed to be the first application of this higher order shell theory to a nonlinear free vibration problem.

The solutions, which reflect the utilization of the Karman-Donnell formulation for a representative assumed modal shape possessing a large or small number of axial waves, reveal the existence of nonperiodic motions. When it is reasonable to assume that the boundary conditions at the shell ends will not significantly affect the frequency of vibration (that is, when the modal shape possesses a large number of axial waves), the nonperiodic solution reflects a lower energy level than the established periodic solution which always implies the boundary condition of "freely supported" ends. When the boundary conditions have a more pronounced effect on the vibration behavior (that is, when the modal shape possesses a small number of axial waves), the resulting motion in the first approximation for "freely supported" ends is again nonperiodic, reflecting, in the present development, an energy level equal to that for the periodic solution. Although the solution corresponding to a small number of axial waves was not the general case under investigation, it may be conjectured that the introduction of a more general deflection function than the one employed will result in a nonperiodic motion reflecting a lower energy level than the periodic solution. For the representative cases investigated herein, the nonperiodic motions for an assumed modal shape possessing either a large or small number of axial waves appear to

be almost periodic. This phenomenon has extreme significance in the interpretation of experimental results. Unfortunately, very little experimental information concerning the nonlinear free vibration behavior of thin shells exists.

When the number of circumferential waves is small, the Karman-Donnell theory becomes invalid and it is necessary to employ a more accurate set of strain-displacement relations, specifically those attributed to Sanders, while at the same time retaining the midsurface inertia terms. Due to the inherent complexity of this nonlinear shell vibration problem, the solution presented herein is based only upon the basic chessboard modal pattern. This then results in a vibration behavior which exhibits pronounced hardening characteristics. Retention of additional terms in the expression for the radial deflection function will permit the possibility of the occurrence of a nonperiodic motion which may, for certain representative cases, appear to be almost periodic, exhibiting either a hardening or a softening characteristic.

For the case when a large number of circumferential waves occurs (Karman-Donnell theory), and for the case when a small number of circumferential waves occurs (Sanders theory), limitations on the two theories are presented based upon the magnitude of the allowable rotations at large displacements. For the free vibration problem, relatively large amplitudes can be tolerated without exceeding limitations on rotation magnitudes.

Future effort on the problem of the vibrating circular cylindrical shell should include the effects of damping and should consider the problem of the nonlinear response of a shell to forced vibration. However, the results of a theoretical development are most beneficial when they can be complementary to the results of an experimental investigation. The future development, as regards the behavior of the nonlinear free and forced vibration of a thin, circular cylindrical shell, will rely heavily upon the findings obtained from experimental studies. Certainly, at the least, the predicted phenomenon of nonperiodic free vibration behavior for the circular cylindrical shells should be verified in the laboratory.

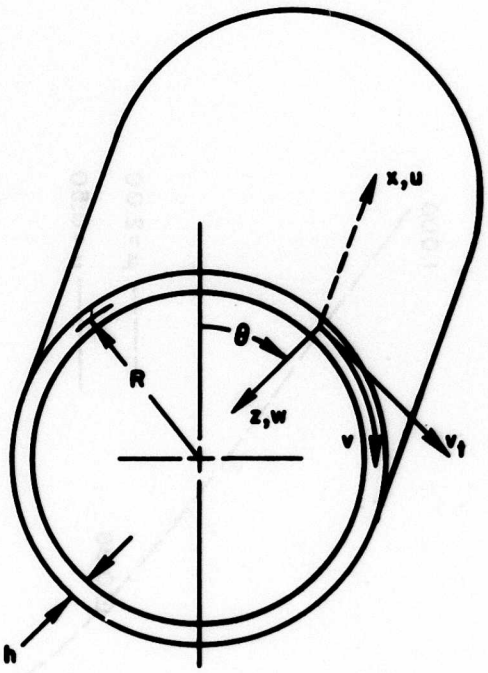

Figure 1. Circular Cylindrical Shell Coordinate System and Sign Convention.

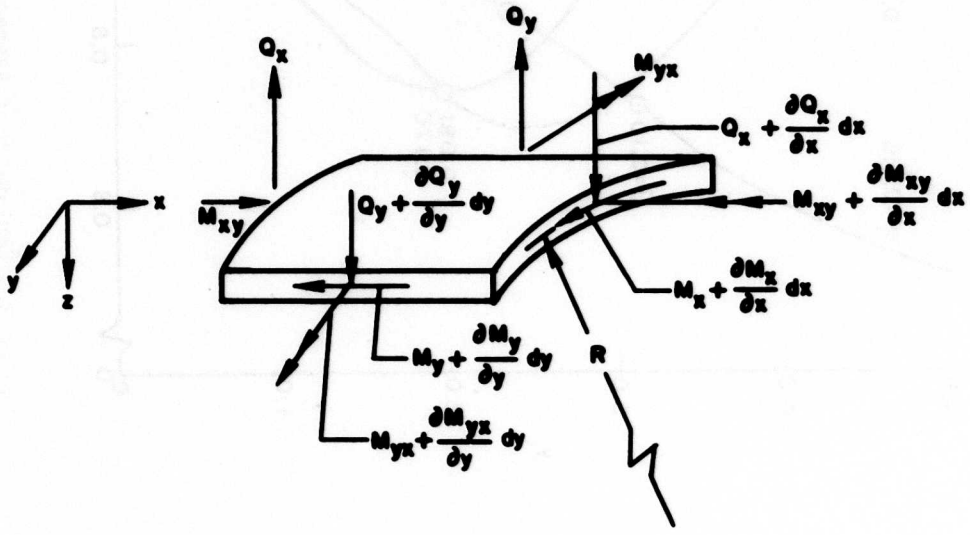

Figure 2. Sign Convention for Shear Forces and Moments Acting on a Shell Element.

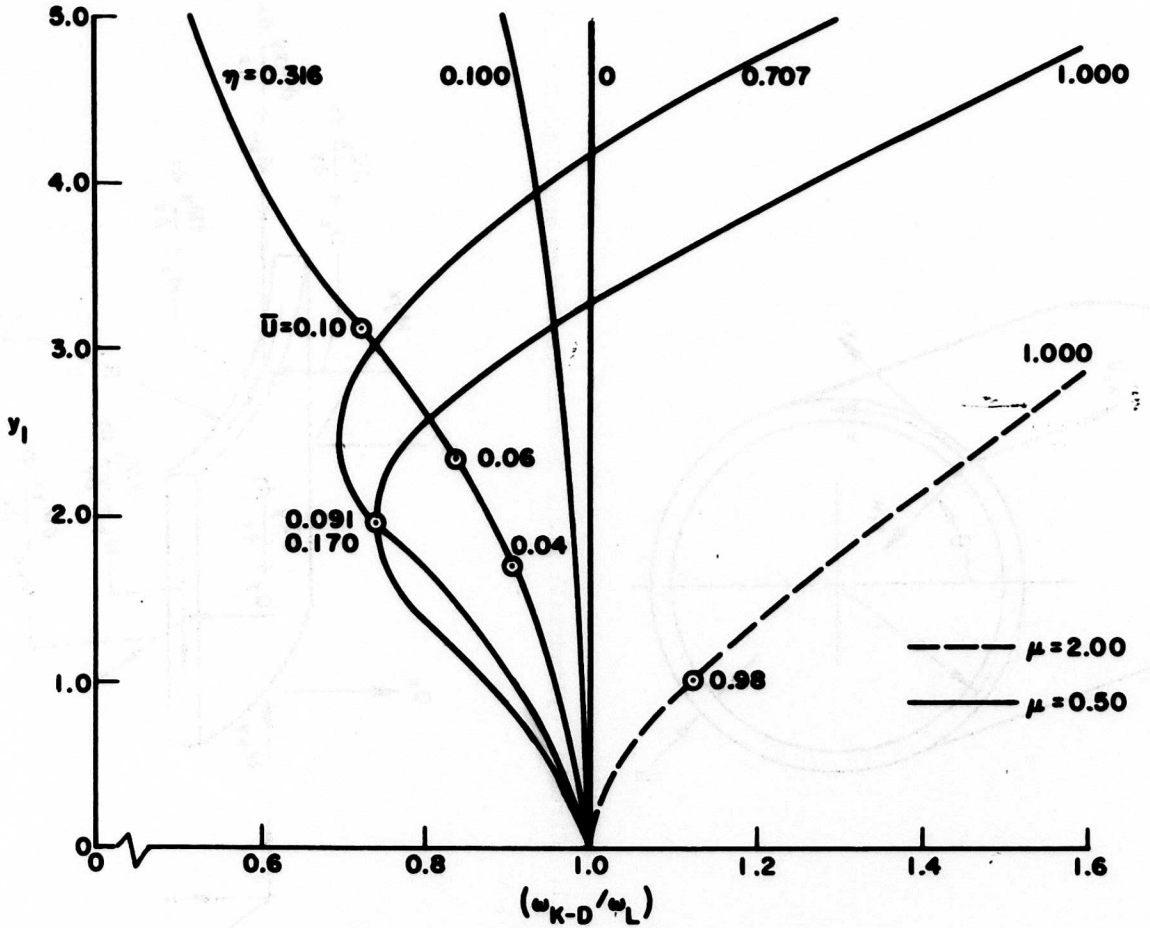

Figure 3. Variation of Average Maximum Displacement With Frequency Ratio for the Fixed Parameter Solution (Reference 16, μ = 0.50 and 2.00).

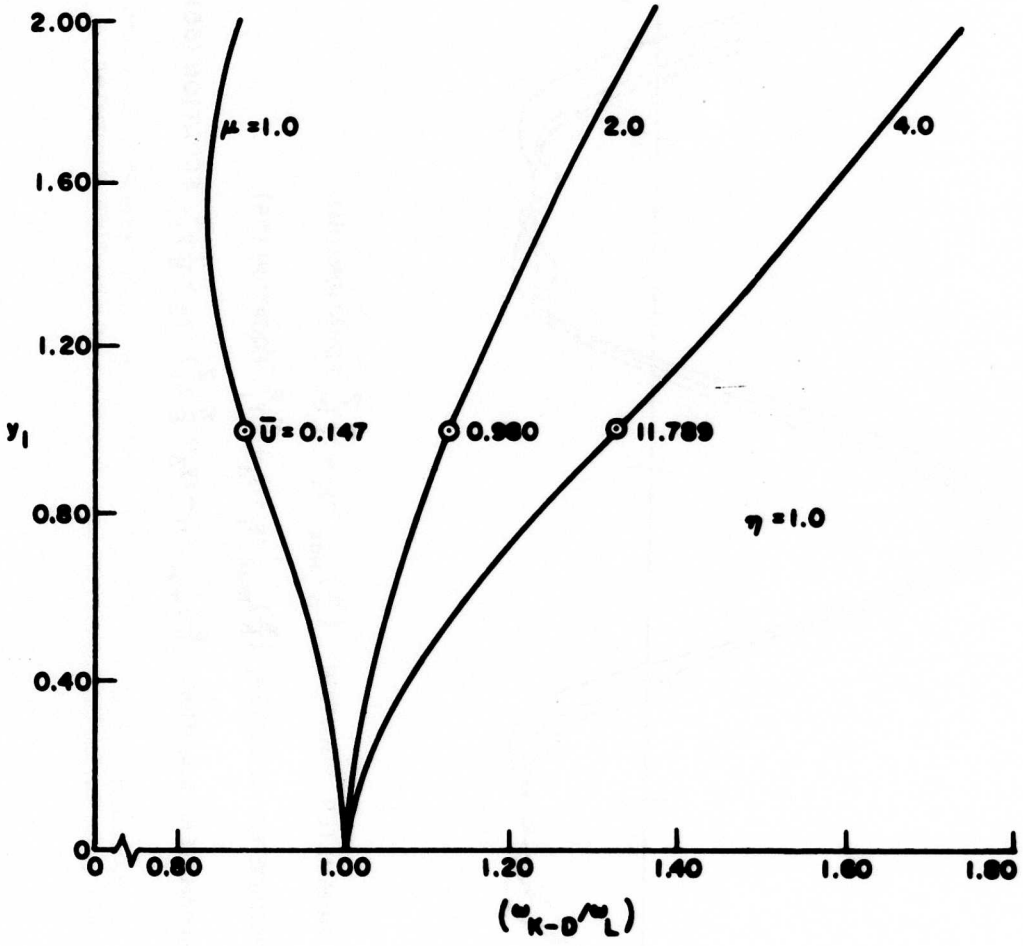

Figure 4. Variation of Average Maximum Displacement With Frequency Ratio for the Fixed Parameter Solution (Reference 16, η = 1.0).

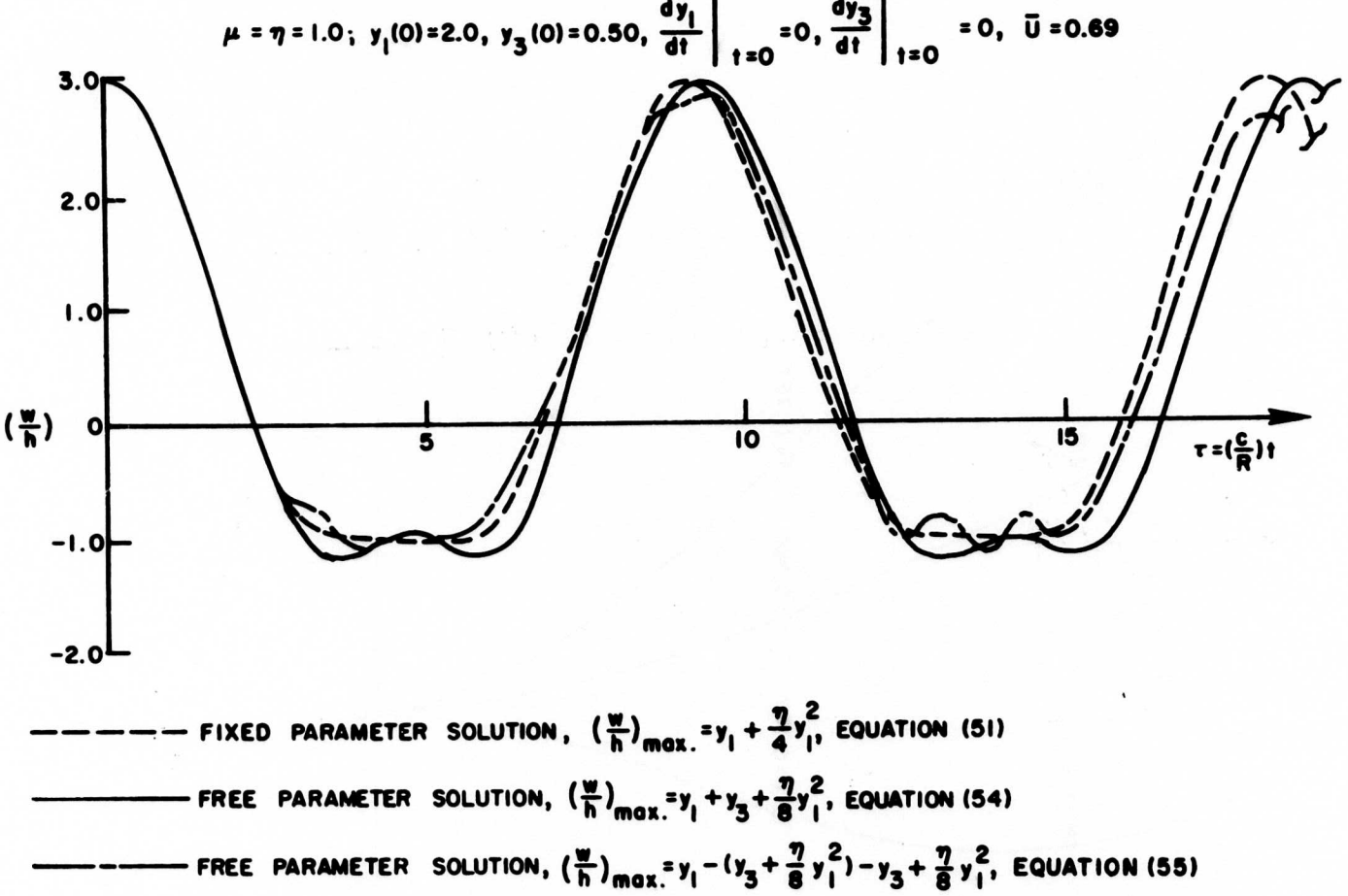

Figure 5. Comparison of the Maximum Radial Displacements for the Fixed Parameter Solution (Reference 16) and the Present Free Parameter Solution as a Function of the Time Parameter τ .

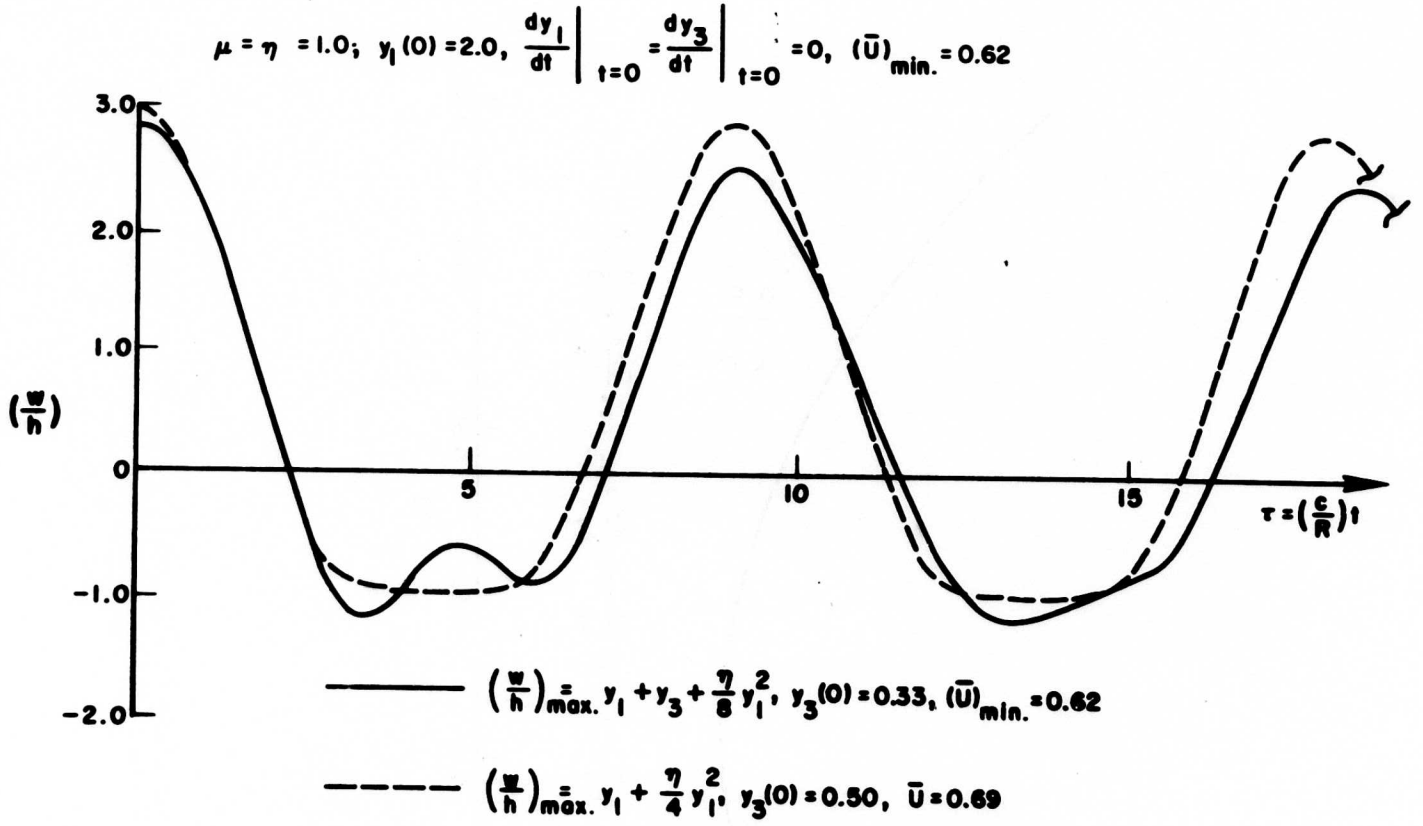

Figure 6. Maximum Radial Displacement for the Present Free Parameter Solution as a Function of the Time Parameter τ for the Minimum Energy Case.

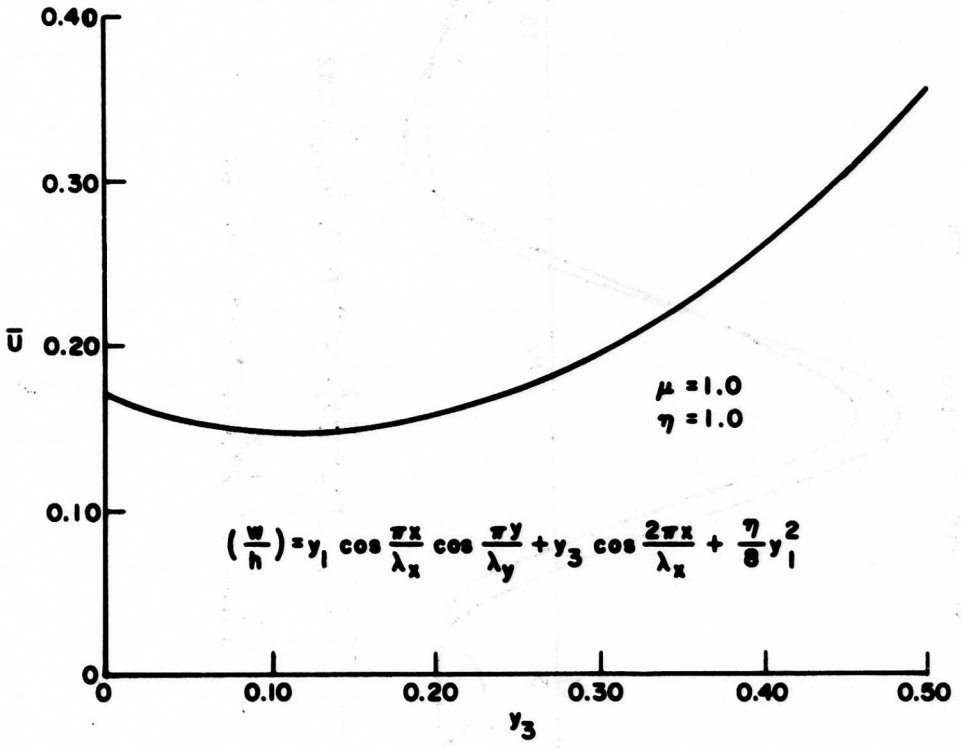

Figure 7. Variation of Strain Energy Parameter With y_3 for the Present Free Parameter Solution ($y_1 = 1.0$).

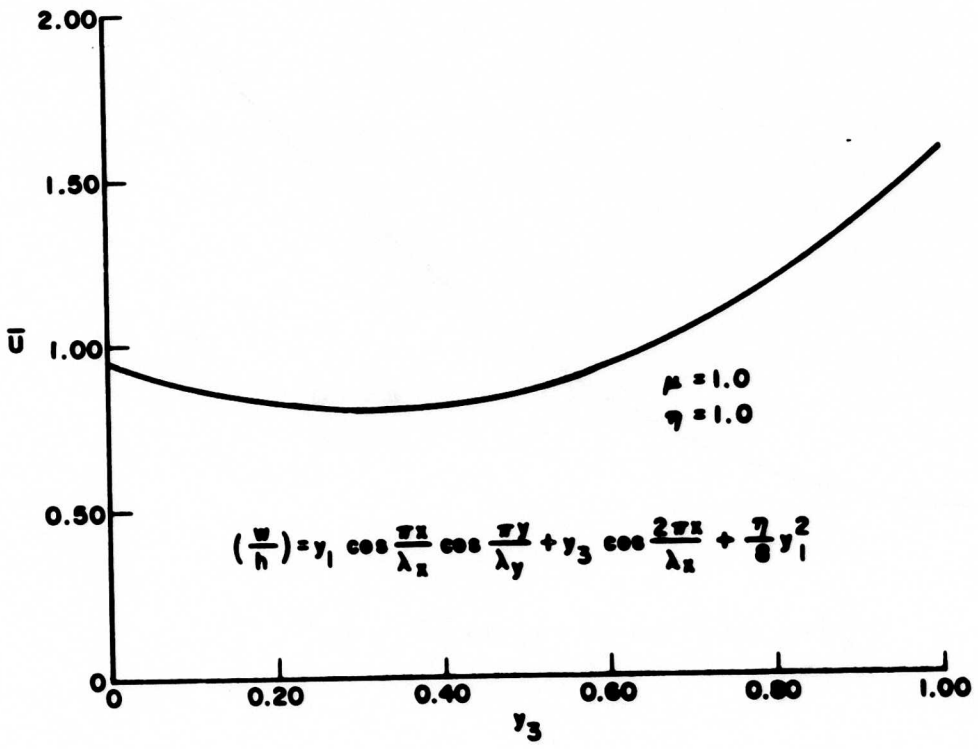

Figure 8. Variation of Strain Energy Parameter With y_3 for the Present Free Parameter Solution ($y_1 = 2.0$).

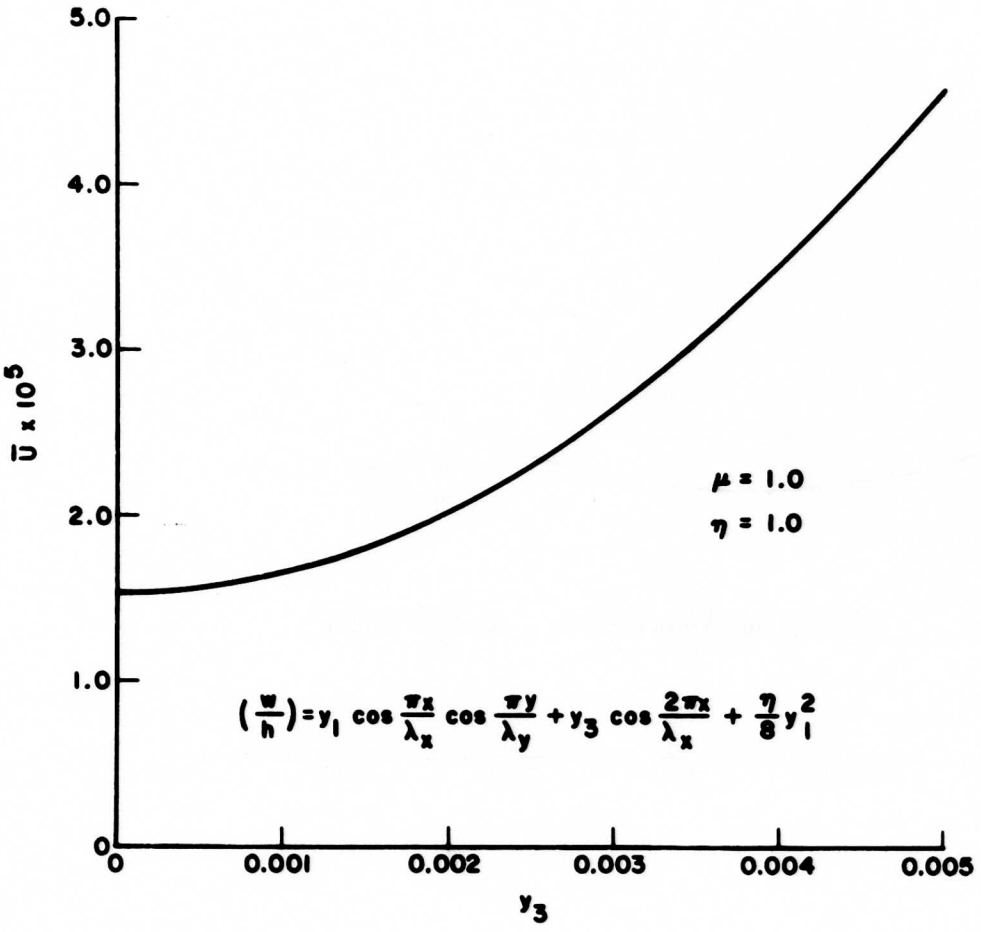

Figure 9. Variation of Strain Energy Parameter With y_3 for the Present Free Parameter Solution ($y_1 = 0.01$).

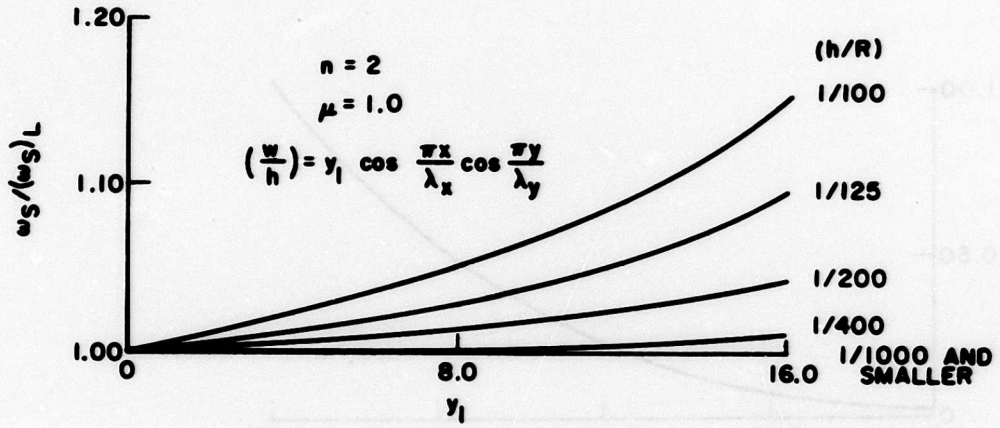

Figure 10. Effect of Finite Deflections on Frequency Ratio Using the Sanders Strain-Displacement Relations (μ = 1.0) .

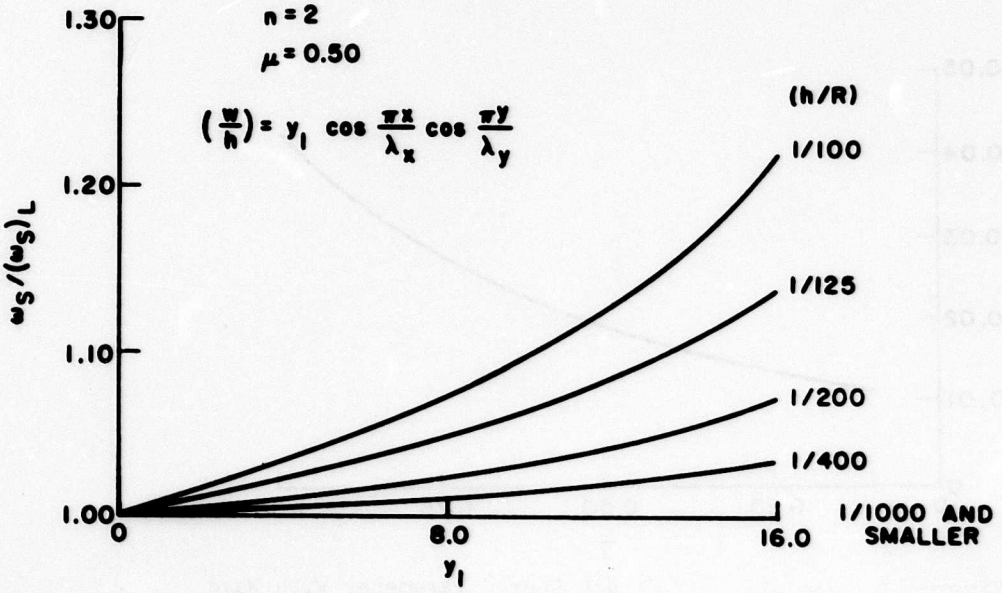

Figure 11. Effect of Finite Deflections on Frequency Ratio Using the Sanders Strain-Displacement Relations (μ = 0.50) .

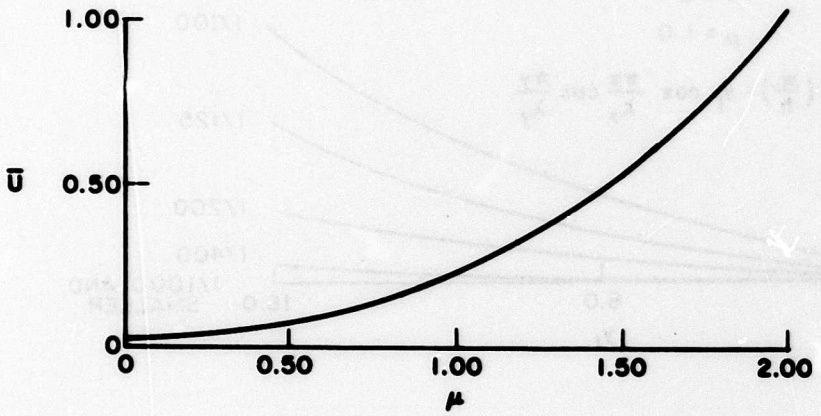

Figure 12. Variation of Strain Energy Parameter With Full Wave Aspect Ratio μ (η = 1.00 , y_1 = 1.00) .

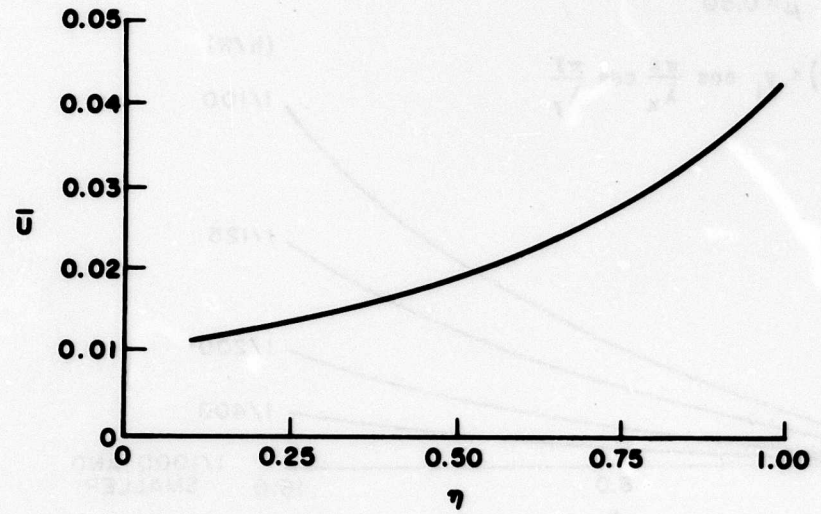

Figure 13. Variation of Strain Energy Parameter With Wave Parameter η (μ = 0.50 , y_1 = 1.00) .

$y_1 = 1.0, \eta = 1.0$

$\mu = 2\lambda_y / 2\lambda_x = 1.0$

$$\left(\frac{w}{h}\right) = y_1 \cos\frac{\pi x}{\lambda_x}\cos\frac{\pi y}{\lambda_y} + \frac{\eta}{8} y_1^2 \cos\frac{2\pi x}{\lambda_x} + \frac{\eta}{8} y_1^2 \quad \text{(REFERENCE 16)}$$

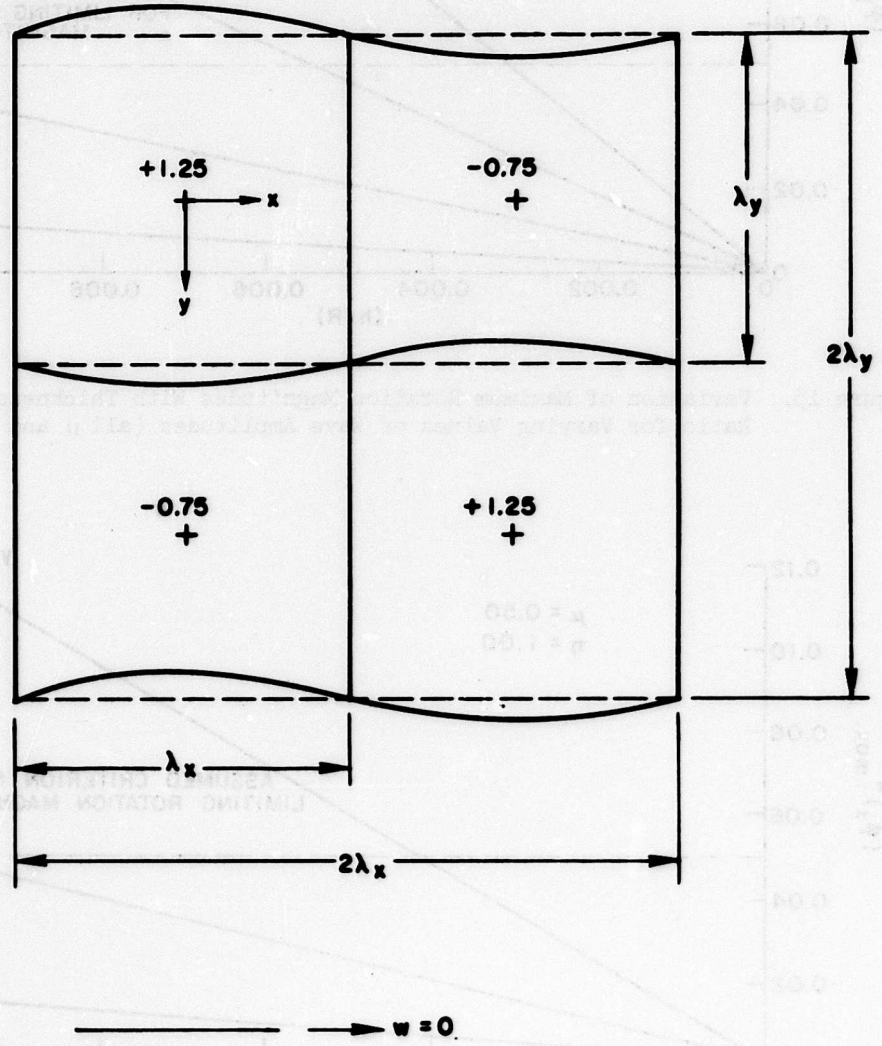

Figure 14. Modal Lines for a Full Wave Aspect Ratio of Unity.

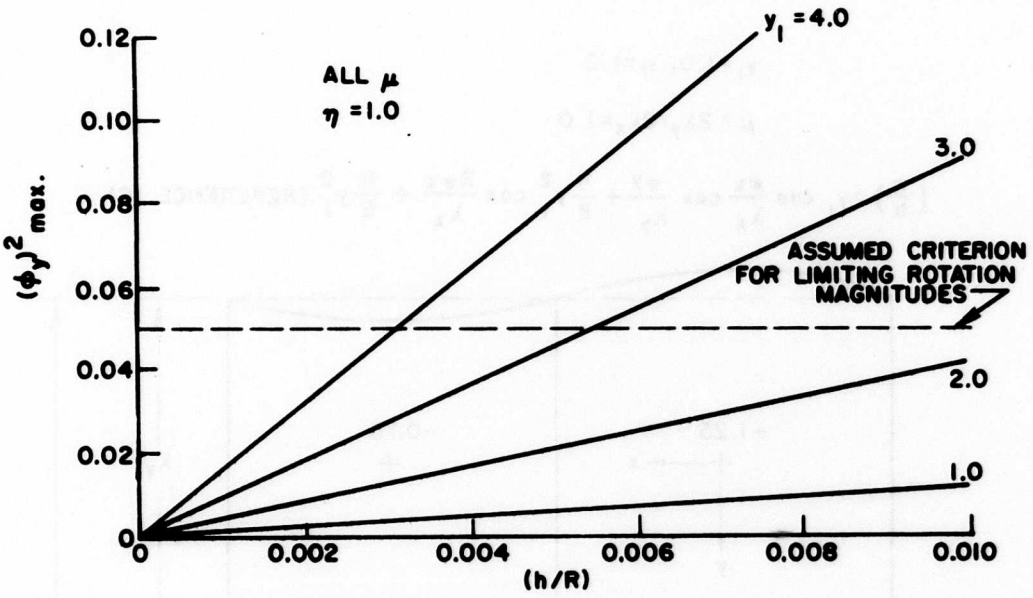

Figure 15. Variation of Maximum Rotation Magnitudes With Thickness-to-Radius Ratio for Varying Values of Wave Amplitudes (all μ and η = 1.0) .

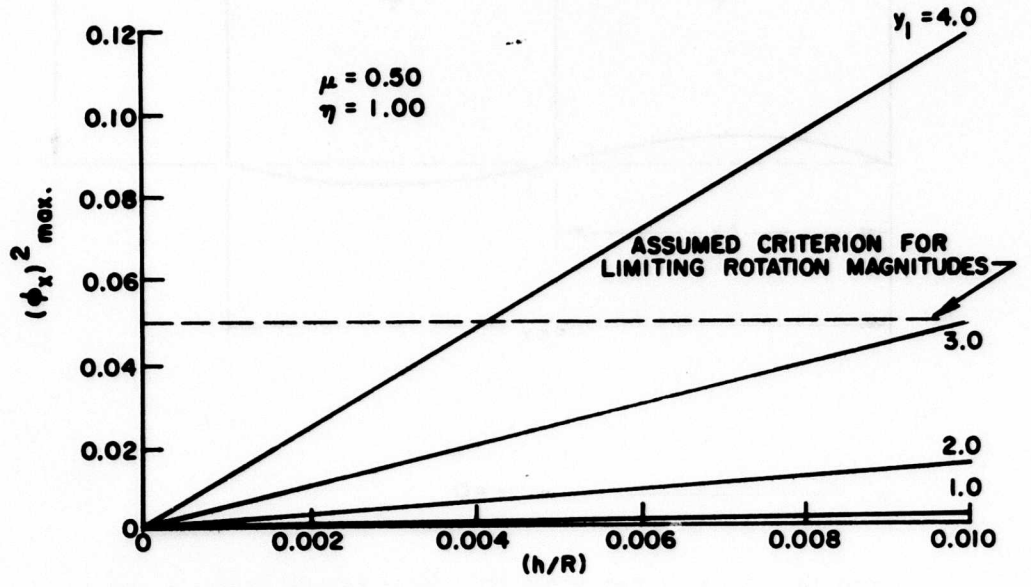

Figure 16. Variation of Maximum Rotation Magnitudes With Thickness-to-Radius Ratio for Varying Values of Wave Amplitudes (μ = 0.50 and η = 1.00) .

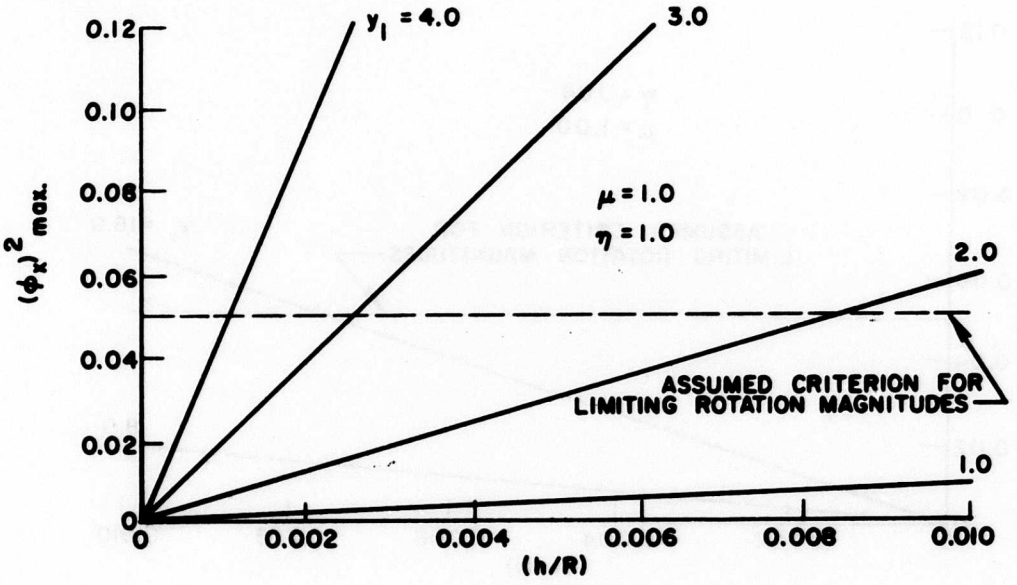

Figure 17. Variation of Maximum Rotation Magnitudes With Thickness-to-Radius Ratio for Varying Values of Wave Amplitudes (μ = 1.0 and η = 1.0) .

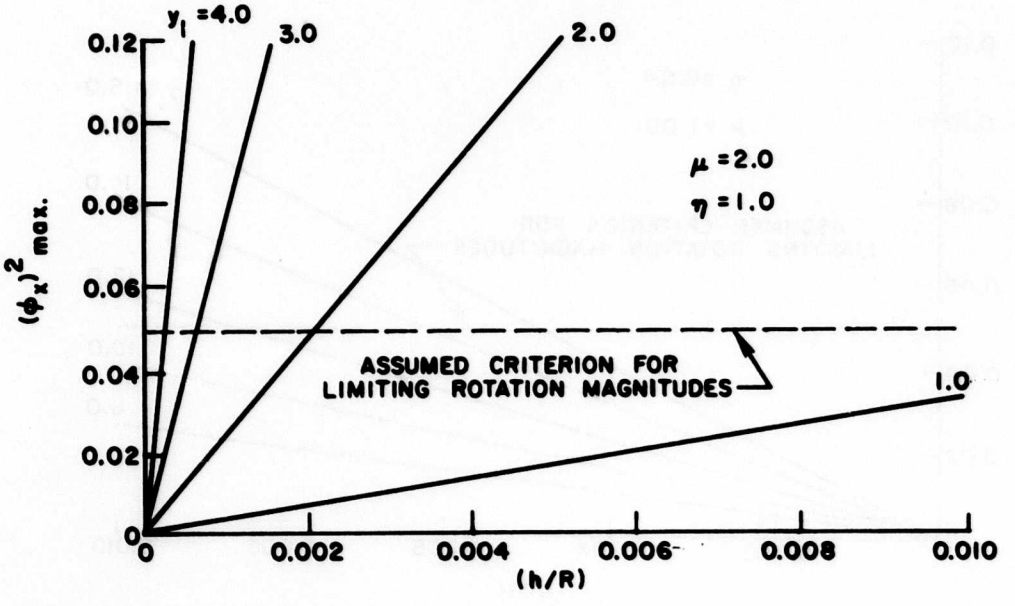

Figure 18. Variation of Maximum Rotation Magnitudes With Thickness-to-Radius Ratio for Varying Values of Wave Amplitudes (μ = 2.0 and η = 1.0) .

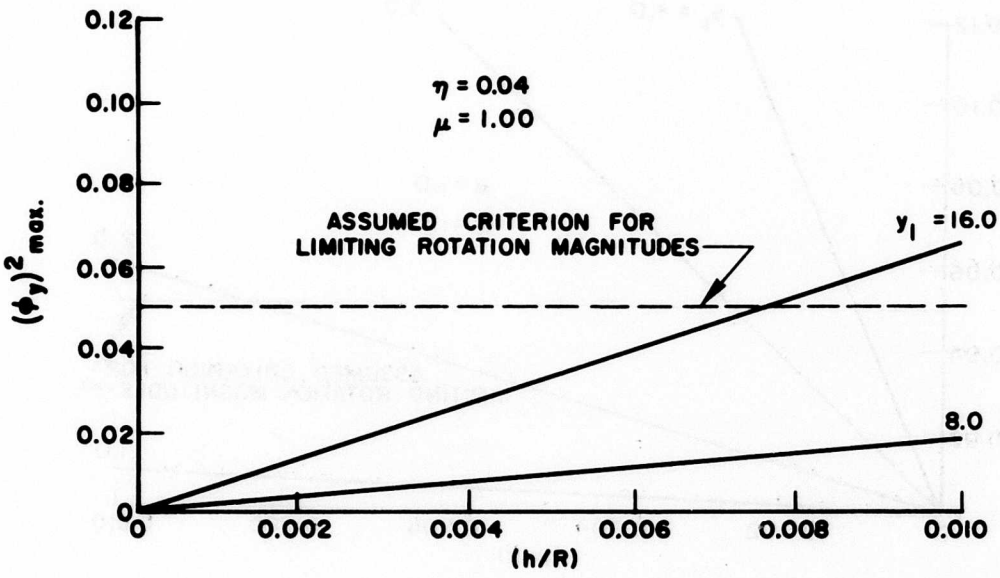

Figure 19. Variation of Maximum Rotation Magnitudes With Thickness-to-Radius Ratio for Varying Values of Wave Amplitudes (μ = 1.00 and η = 0.04) .

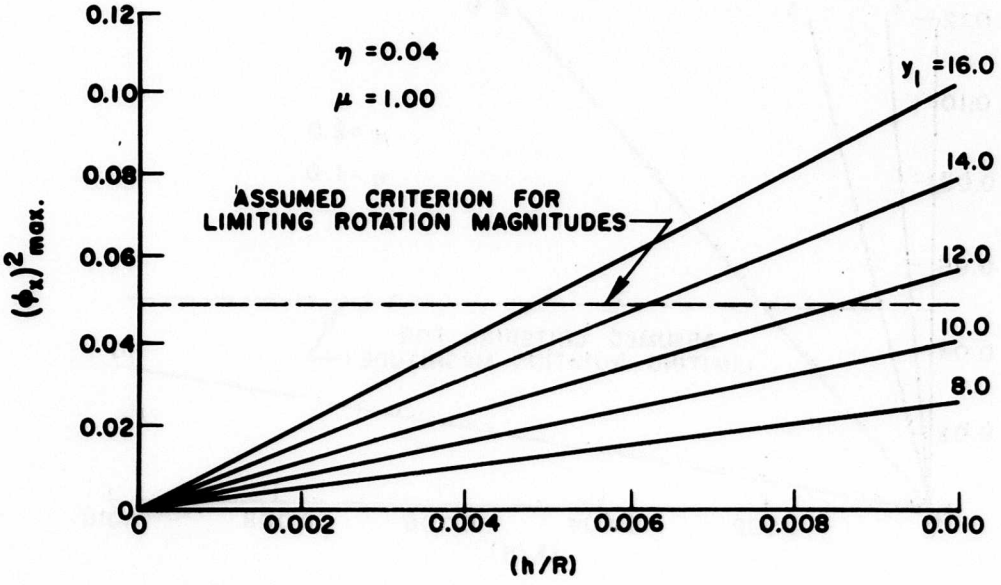

Figure 20. Variation of Maximum Rotation Magnitudes With Thickness-to-Radius Ratio for Varying Values of Wave Amplitudes (μ = 1.00 and η = 0.04) .

REFERENCES

1. Rayleigh, J. W. S., THEORY OF SOUND, Second Edition, New York, the MacMillan Company, Vol. 1, p. 403.

2. Love, A. E. H., A TREATISE ON THE MATHEMATICAL THEORY OF ELASTICITY, Fourth Edition, New York, Dover Publications, p. 543.

3. Flügge, W., STATIK UND DYNAMIK DER SCHALEN, Germany, Springer-Verlag, pp. 115 and 230.

4. Arnold, R. N., and Warburton, G. B., FLEXURAL VIBRATIONS OF THE WALLS OF THIN CYLINDRICAL SHELLS HAVING FREELY SUPPORTED ENDS, Proceedings of the Royal Society, Series A, Vol. 197, 1949, pp. 238-256.

5. Arnold, R. N., and Warburton, G. B., THE FLEXURAL VIBRATIONS OF THIN CYLINDERS, Proceedings of the Institution of Mechanical Engineers, Series A, Vol. 167, 1953, pp. 62-80.

6. Reissner, E., ON TRANSVERSE VIBRATIONS OF THIN, SHALLOW ELASTIC SHELLS, Quarterly of Applied Mathematics, Vol. 13, 1955, pp. 169-176.

7. Donnell, L. H., A NEW THEORY FOR THE BUCKLING OF THIN CYLINDERS UNDER AXIAL COMPRESSION AND BENDING, Transactions of the American Society of Mechanical Engineers, Vol. 56, November 1934, pp. 795-806.

8. Reissner, E., NON-LINEAR EFFECTS IN VIBRATIONS OF CYLINDRICAL SHELLS, Ramo-Wooldridge Corporation, Aeromechanics Report No. 5-6, Redondo Beach, California, 1955.

9. Gottenberg, W. G., EXPERIMENTAL STUDY OF THE VIBRATIONS OF A CIRCULAR CYLINDRICAL SHELL, Journal of the Acoustical Society of America, Vol. 32, 1960, pp. 1002-1006.

10. Koval, L. R., and Cranch, E. T., ON THE FREE VIBRATIONS OF THIN CYLINDRICAL SHELLS SUBJECTED TO AN INITIAL STATIC TORQUE, Fourth U.S. National Congress of Applied Mechanics, Vol. 1, 1962, pp. 107-117.

11. Koval, L. R., NOTE ON THE VIBRATIONAL CHARACTERISTICS OF THIN WALLED SHELLS, AIAA Journal, Vol. 4, No. 3, 1966, pp. 571-572.

12. Karman, T. von, and Tsien, H. S., THE BUCKLING OF THIN CYLINDRICAL SHELLS UNDER AXIAL COMPRESSION, Journal of the Aeronautical Sciences, Vol. 8, No. 8, 1941, pp. 303-312.

13. Evensen, D. A., SOME OBSERVATIONS ON THE NONLINEAR VIBRATION OF THIN CYLINDRICAL SHELLS, AIAA Journal, Vol. 1, No. 12, 1963, pp. 2857-2858.

14. Chu, H N., INFLUENCE OF LARGE AMPLITUDES ON FLEXURAL VIBRATIONS OF A THIN CIRCULAR CYLINDRICAL SHELL, Journal of the Aerospace Sciences, Vol. 28, No. 8, 1961, pp. 602-609.

15. Nowinski, J., NONLINEAR TRANSVERSE VIBRATIONS OF ORTHOTROPIC CYLINDRICAL SHELLS, AIAA Journal, Vol. 1, 1963, pp. 617-620.

16. Evensen, D. A., and Fulton, R. E., DYNAMIC STABILITY OF STRUCTURES, (Proceedings of an International Conference, Evanston, Illinois, October 18-20, 1965), London, Pergamon Press, 1967, pp. 237-254.

17. Olson, M. D., SOME EXPERIMENTAL OBSERVATIONS ON THE NONLINEAR VIBRATION OF CYLINDRICAL SHELLS, AIAA Journal, Vol. 3, No. 9, 1965, pp. 1775-1777.

18. Sanders, J. L., NONLINEAR THEORIES OF THIN SHELLS, Quarterly of Applied Mathematics, Vol. 21, 1963, pp. 21-36.

19. Mayers, J. and Rehfield, L. W., DEVELOPMENTS IN MECHANICS, Vol. 3, Part 1 (Proceedings of the Ninth Midwestern Mechanics Conference, Madison, Wisconsin, August 16-18, 1965), New York, John Wiley and Sons, Inc., 1967, pp. 145-160.

20. Sanders, J. L., AN IMPROVED FIRST-APPROXIMATION THEORY FOR THIN SHELLS, National Advisory Committee for Aeronautics, NACA TR R-24, Washington, D.C., 1960.

21. Leggett, D. M. A., and Jones, R. P. N., THE BEHAVIOR OF A CYLINDRICAL SHELL UNDER AXIAL COMPRESSION WHEN THE BUCKLING LOAD HAS BEEN EXCEEDED, Technical Report of the Aeronautical Research Committee, Vol. II, No. 60, 1942, pp. 779-784, Report and Memoranda No. 2190.

22. Kempner, J., POSTBUCKLING BEHAVIOR OF AXIALLY COMPRESSED CIRCULAR CYLINDRICAL SHELLS, Journal of the Aeronautical Sciences, Vol. 21, No. 5, 1954, pp. 329-336.

APPENDIX I

DEVELOPMENT OF THE APPROXIMATE SOLUTION FOR A LARGE NUMBER OF CIRCUMFERENTIAL WAVES FOR THE FIXED PARAMETER CASE

This appendix presents a step-by-step development leading to the solution presented and discussed in earlier sections.

The governing differential equations were developed earlier and are listed again as

$$D\nabla^4 w - h\left(\frac{\partial^2 F}{\partial y^2}\frac{\partial^2 w}{\partial x^2} + \frac{\partial^2 F}{\partial x^2}\frac{\partial^2 w}{\partial y^2} - 2\frac{\partial^2 F}{\partial x \partial y}\frac{\partial^2 w}{\partial x \partial y}\right) - \left(\frac{h}{R}\right)\frac{\partial^2 F}{\partial x^2} = -\rho h \frac{\partial^2 w}{\partial t^2} \qquad (57)$$

and

$$\nabla^4 F = E\left[\left(\frac{\partial^2 w}{\partial x \partial y}\right)^2 - \frac{\partial^2 w}{\partial x^2}\frac{\partial^2 w}{\partial y^2}\right] - \left(\frac{E}{R}\right)\frac{\partial^2 w}{\partial x^2} \qquad (58)$$

The deflection function for a shell vibrating in the nth mode is given by

$$\left(\frac{w}{h}\right) = y_1(t)\cos\frac{\pi x}{\lambda_x}\cos\frac{\pi y}{\lambda_y} + \frac{\eta}{8}y_1^2(t)\cos\frac{2\pi x}{\lambda_x} + \frac{\eta}{8}y_1^2(t) \qquad (59)$$

Substitution of the deflected shape into Equation (58) and subsequent solution yield the following expression for the stress function:

$$F = -\frac{2Eh^2\mu^2}{(1+\mu^2)^2}\left(+\frac{\eta}{8}y_1^3 - \frac{1}{2\eta}y_1\right)\cos\frac{\pi x}{\lambda_x}\cos\frac{\pi y}{\lambda_y}$$

$$-\frac{2Eh^2\mu^2}{(1+9\mu^2)^2}\frac{\eta}{8}y_1^3\cos\frac{3\pi x}{\lambda_x}\cos\frac{\pi y}{\lambda_y} - \frac{Eh^2\mu^2}{32}y_1^2\cos\frac{2\pi y}{\lambda_y} \qquad (60)$$

The deflection function and the stress function given by Equations (59) and (60) lead to satisfaction of the requirement that the circumferential displacement be a periodic function of the circumferential coordinate.

The Lagrangian ($L \equiv T-U$) can be written as follows:

$$(U-T) = \frac{h}{2E} \int_0^{\ell} \int_0^{2\pi R} \left[(\sigma_x + \sigma_y)^2 - 2(1+\nu)\,(\sigma_x \sigma_y - \tau_{xy}^2) \right] dxdy$$

$$+ \frac{D}{2} \int_0^{\ell} \int_0^{2\pi R} \left[\left(\frac{\partial^2 w}{\partial x^2} \right)^2 + \left(\frac{\partial^2 w}{\partial y^2} \right)^2 + 2\nu \frac{\partial^2 w}{\partial x^2} \frac{\partial^2 w}{\partial y^2} + 2(1-\nu) \left(\frac{\partial^2 w}{\partial x \partial y} \right)^2 \right] dxdy$$

$$- \frac{\rho h}{2} \int_0^{\ell} \int_0^{2\pi R} \left(\frac{\partial w}{\partial t} \right)^2 dxdy \qquad (61)$$

The relations between the stresses and the stress function are given by Equation (48). Substitution of the deflected shape and the stress function into Equation (61) for the Lagrangian, after integration over x and y, yields

$$\bar{L} = \left(\frac{\pi E h^3 \ell}{R} \right)^{-1} (U-T) = \frac{\mu^4}{4} \left\{ + \frac{\eta^4}{16} \frac{y_1^6}{(1+9\mu^2)^2} + \frac{4}{(1+\mu^2)^2} \left(+ \frac{\eta^2 y_1^3}{8} - \frac{1}{2} y_1 \right)^2 \right.$$

$$\left. + \frac{\eta^2 y_1^4}{32} \right\} + \frac{\eta^2 \mu^4}{48(1-\nu^2)} \left(+ y_1^2 + \frac{\eta^2}{2} y_1^4 \right) + \frac{\eta^2}{48(1-\nu^2)} y_1^2 + \frac{\eta^2 \mu^2}{24(1-\nu^2)} y_1^2$$

$$- \frac{1}{4} \left(\frac{\rho c^2}{E} \right) \left(\frac{dy_1}{d\tau} \right)^2 \left(1 + \frac{3\eta^2}{8} y_1^2 \right) \qquad (62)$$

where τ is a nondimensional independent variable related to the time t by the following relation:

$$\tau = \frac{c}{R} t \qquad (63)$$

The application of the variational principle relative to $y_1(\tau)$ yields

the following Euler equation:

$$\frac{d^2y_1}{d\tau^2} = -\frac{1}{\left(+2+\frac{3}{4}\eta^2y_1^2\right)}\left\{+\frac{3}{4}\eta^2y_1\left(\frac{dy_1}{d\tau}\right)^2+4\left(\frac{E}{\rho c^2}\right)\left[+\frac{\eta^2\mu^4}{4}\times\right.\right.$$

$$\left[+\frac{3\eta^2}{8(1+9\mu^2)^2}y_1^5+\frac{8}{(1+\mu^2)^2}\left(+\frac{\eta y_1^3}{8}-\frac{1}{2\eta}y_1\right)\left(+\frac{3\eta y_1^2}{8}-\frac{1}{2\eta}\right)\right.$$

$$\left.\left.\left.+\frac{y_1^3}{8}\right]+\frac{\eta^2\mu^4}{48(1-\nu^2)}\left(+2y_1+2\eta^2y_1^3\right)+\frac{\eta^2}{24(1-\nu^2)}y_1+\frac{\eta^2\mu^2}{12(1-\nu^2)}y_1\right]\right\} \quad (64)$$

Equation (64) is a single second-order differential equation in the independent variable τ. By making a change of variable, the single second-order differential equation in τ is reduced to two coupled first-order differential equations in τ. The required change of variable is given by

$$\frac{dy_1}{d\tau} = y_2 \quad (65)$$

Then, the two coupled first-order equations in τ become

$$\frac{dy_1}{d\tau} = y_2 \quad (66)$$

and

$$\frac{dy_2}{d\tau} = -\frac{1}{\left(+2+\frac{3}{4}\eta^2y_1^2\right)}\left\{+\frac{3}{4}\eta^2y_1y_2^2+4\left(\frac{E}{\rho c^2}\right)\left[+\frac{\eta^2\mu^4}{4}\times\right.\right.$$

$$\left[+\frac{3\eta^2}{8(1+9\mu^2)^2}y_1^5+\frac{8}{(1+\mu^2)^2}\left(+\frac{\eta y_1^3}{8}-\frac{1}{2\eta}y_1\right)\left(+\frac{3\eta y_1^2}{8}-\frac{1}{2\eta}\right)+\frac{y_1^3}{8}\right]$$

$$\left.\left.+\frac{\eta^2\mu^4}{48(1-\nu^2)}\left(+2y_1+2\eta^2y_1^3\right)+\frac{\eta^2}{24(1-\nu^2)}y_1+\frac{\eta^2\mu^2}{12(1-\nu^2)}y_1\right]\right\} \quad (67)$$

Solution of the two coupled differential equations was carried out by standard numerical techniques in conjunction with utilization of the Burroughs 5500 computer in the Stanford University Computation Center.

APPENDIX II

DEVELOPMENT OF THE APPROXIMATE SOLUTION FOR A LARGE NUMBER OF CIRCUMFERENTIAL WAVES FOR THE FREE PARAMETER CASE

This appendix presents a step-by-step development of the solution when the assumed deflected shape is more general than that used in Appendix I.

The deflection function is given by

$$\left(\frac{w}{h}\right) = y_1(t) \cos\frac{\pi x}{\lambda_x} \cos\frac{\pi y}{\lambda_y} + y_3(t) \cos\frac{2\pi x}{\lambda_x} + y_5(t) \tag{68}$$

The stress function, obtained as in Appendix I, is given by

$$\begin{aligned} F = & -\frac{2Eh^2\mu^2}{(1+\mu^2)^2}\left(+y_1y_3 - \frac{1}{2\eta}y_1\right)\cos\frac{\pi x}{\lambda_x}\cos\frac{\pi y}{\lambda_y} \\ & -\frac{2Eh^2\mu^2}{(1+9\mu^2)^2}y_1y_3\cos\frac{3\pi x}{\lambda_x}\cos\frac{\pi y}{\lambda_y} - \frac{Eh^2}{16\mu^2}\left(+\frac{y_1^2}{2}+\frac{4}{\eta}y_3\right)\cos\frac{2\pi x}{\lambda_x} \\ & -\frac{Eh^2\mu^2}{32}y_1^2\cos\frac{2\pi y}{\lambda_y} \end{aligned} \tag{69}$$

The continuity condition for the circumferential displacement is given by the following mathematical representation:

$$\int_0^{2\pi R}\frac{\partial v}{\partial y}\,dy = \int_0^{2\pi R}\left[\frac{1}{E}\left(\frac{\partial^2 F}{\partial x^2} - \nu\frac{\partial^2 F}{\partial y^2}\right) + \frac{w}{R} - \frac{1}{2}\left(\frac{\partial w}{\partial y}\right)^2\right]dy = 0 \tag{70}$$

Substitution of the deflected shape and the stress function into the continuity condition yields the following relation:

$$y_5 = \frac{\eta}{8}y_1^2 \tag{71}$$

Hence, the deflected shape now becomes

$$\left(\frac{w}{h}\right) = y_1(t) \cos\frac{\pi x}{\lambda_x} \cos\frac{\pi y}{\lambda_y} + y_3(t) \cos\frac{2\pi x}{\lambda_x} + \frac{\eta}{8}y_1^2(t) \tag{72}$$

Substitution of the deflected shape and the stress function into the Lagrangian (in a manner exactly analogous to that described in Appendix I) after integration over x and y yields

$$\bar{L} = \left(\frac{\pi E h^3 \ell}{R}\right)^{-1} (U-T) = \frac{1}{4}\left\{+\frac{4\mu^4\eta^2}{(1+9\mu^2)^2} y_1^2 y_3^2 + \frac{4\mu^4}{(1+\mu^2)^2}\left(+\eta y_1 y_3 - \frac{1}{2} y_1\right)^2\right.$$

$$\left. + \frac{\eta^2\mu^4}{32} y_1^4 + \frac{1}{8}\left(+\frac{\eta y_1^2}{2} - 4y_3\right)^2\right\} + \frac{\eta^2\mu^4}{48(1-\nu^2)} (+ y_1^2 + 32 y_3^2)$$

$$+ \frac{\eta^2}{48(1-\nu^2)} y_1^2 + \frac{1}{24(1-\nu^2)} \eta^2\mu^2 y_1^2 - \frac{1}{4}\left(\frac{\rho c^2}{E}\right)\left[\left(\frac{dy_1}{d\tau}\right)^2\left(1 + \frac{\eta^2}{4} y_1^2\right)\right.$$

$$\left. + 2\left(\frac{dy_3}{d\tau}\right)^2\right] \qquad (73)$$

The application of the variational principle, relative to $y_1(\tau)$ and $y_3(\tau)$, yields two Euler equations. After the introduction of two changes of variable defined by

$$\frac{dy_1}{d\tau} = y_2 \qquad (74)$$

and

$$\frac{dy_3}{d\tau} = y_4 \qquad (75)$$

the two second-order Euler differential equations are transformed into four first-order differential equations. The first two are given by Equations (74) and (75). The remaining two equations are

$$\frac{dy_2}{d\tau} = -\frac{1}{\left(+2 + \frac{\eta^2}{2} y_1^2\right)}\left\{+\frac{\eta^2}{2} y_1 y_2^2 + \frac{4E}{\rho c^2}\left[+\frac{\eta^2}{4}\left[+\frac{8\mu^4 y_1 y_2^2}{(1+9\mu^2)^2}\right.\right.\right.$$

$$\left.\left.\left. + \frac{8\mu^4}{(1+\mu^2)^2}\left(+ y_1 y_3 - \frac{1}{2\eta} y_1\right)\left(+ y_3 - \frac{1}{2\eta}\right) + \frac{\mu^4}{8} y_1^3\right.\right.\right.$$

(Continued)

$$+ \frac{1}{4}\left(+\frac{y_1^2}{2} - \frac{4}{\eta} y_3\right) y_1\Bigg] + \frac{\eta^2\mu^4}{24(1-\nu^2)} y_1 + \frac{\eta^2}{24(1-\nu^2)} y_1 + \frac{\eta^2\mu^2}{12(1-\nu^2)}\Bigg]\Bigg\} \tag{76}$$

and

$$\frac{dy_4}{d\tau} = -\left(\frac{E}{\rho c^2}\right)\Bigg\{+\frac{\eta^2}{4}\Bigg[+\frac{8\mu^4 y_1^2 y_3}{(1+\mu^2)^2} + \frac{8\mu^4}{(1+\mu^2)^2}\left(y_1 y_3 - \frac{1}{2} y_1\right)$$

$$- \frac{1}{\eta}\left(+\frac{y_1^2}{2} - \frac{4}{\eta} y_3\right)\Bigg] + \frac{4}{3}\frac{\eta^2\mu^4}{(1-\nu^2)} y_3\Bigg\} \tag{77}$$

Solution of the four coupled differential equations was carried out by standard numerical techniques in conjunction with utilization of the Burroughs 5500 computer in the Stanford University Computation Center.

APPENDIX III

DEVELOPMENT OF THE APPROXIMATE SOLUTION FOR A SMALL NUMBER OF CIRCUMFERENTIAL WAVES

This appendix presents the development of the differential equations of motion by the use of the strain-displacement relations deduced by Sanders.

The deflection functions are given by

$$\left.\begin{aligned}
\left(\frac{w}{n}\right) &= y_1(t)\cos\frac{\pi x}{\lambda_x}\cos\frac{\pi y}{\lambda_y} \\
n\left(\frac{u}{h}\right) &= y_3(t)\sin\frac{\pi x}{\lambda_x}\cos\frac{\pi y}{\lambda_y} + y_5(t)\sin\frac{2\pi x}{\lambda_x}\cos\frac{2\pi y}{\lambda_y} + y_7(t)\sin\frac{2\pi x}{\lambda_x} \\
n\left(\frac{v}{h}\right) &= y_9(t)\cos\frac{\pi x}{\lambda_x}\sin\frac{\pi y}{\lambda_y} + y_{11}(t)\cos\frac{2\pi x}{\lambda_x}\sin\frac{2\pi y}{\lambda_y} + y_{13}(t)\sin\frac{2\pi y}{\lambda_y}
\end{aligned}\right\} \quad (78)$$

Substitution of the deflected shapes into the strain energy and the kinetic energy expressions (Equations (17) and (18), respectively) after integration over x and y yields the following expression for the Lagrangian:

$$\bar{L} = L\left(\frac{\pi Eh^3\ell}{R}\right)^{-1} = \left(\frac{\pi Eh^3\ell}{R}\right)^{-1}(U-T)$$

$$= \frac{1}{4(1-\nu^2)}\left\{+\mu^2y_3^2 + \left(+2\mu y_5 - \frac{1}{8}\eta\mu^2y_1^2\right)^2 + 8\mu^2y_7^2 - \mu^3\eta y_7y_1^2\right.$$

$$+ \frac{\mu^4\eta^2}{8}y_1^4 + 6\left[+\frac{\eta}{8}y_1^2 - \left(\frac{h}{R}\right)\frac{y_1y_9}{4}\right]^2 + 2\left[+2y_{13} - \frac{\eta}{8}y_1^2 + \left(\frac{h}{R}\right)\frac{y_1y_9}{4}\right]^2$$

$$\left.+ \frac{3}{16}\left(\frac{h}{R}\right)^2y_1^2y_{11}^2 + \left[+2y_{11} - \frac{\eta}{8}y_1^2 + \left(\frac{h}{R}\right)\frac{y_1y_9}{4}\right]^2\right.$$

(Continued)

$$+\left[+y_9 - y_1 - \left(\frac{h}{R}\right)\frac{y_1y_{11}}{4} - \left(\frac{h}{R}\right)\frac{y_1y_{13}}{2}\right]^2 + \frac{1}{4}\left(\frac{h}{R}\right)^2 y_1^2y_{11}y_{13}$$

$$+ \frac{1}{4}\left(\frac{h}{R}\right)^2 y_1^2y_{13}^2 + 2\nu\left[+\mu y_3\left[+y_7 - y_1 - \left(\frac{h}{R}\right)\frac{y_1y_{11}}{4} - \left(\frac{h}{R}\right)\frac{y_1y_{13}}{2}\right]\right.$$

$$+\left(+2\mu y_5 - \frac{\eta\mu^2}{8}y_1^2\right)\left[+2y_{11} - \frac{\eta}{8}y_1^2 + \left(\frac{h}{R}\right)\frac{y_1y_{11}}{4}\right] + 2\left(+2\mu y_7\right.$$

$$\left.- \frac{\eta\mu^2}{8}y_1^2\right)\left[+\frac{\eta}{8}y_1^2 - \left(\frac{h}{R}\right)\frac{y_1y_9}{4}\right] + \frac{\eta\mu^2}{4}y_1^2\left[+2y_{13} - \frac{\eta}{8}y_1^2 + \left(\frac{h}{R}\right)\frac{y_1y_9}{4}\right]$$

$$+ \frac{\eta\mu^2}{2}y_1^2\left[+\frac{\eta}{8}y_1^2 - \left(\frac{h}{R}\right)\frac{y_1y_9}{4}\right]\Bigg] + \frac{(1-\nu)}{2}\left[+\left[-y_3 - \mu y_9\right.\right.$$

$$\left.- \left(\frac{h}{R}\right)\frac{\mu y_1y_{13}}{2} + \left(\frac{h}{R}\right)\frac{\mu y_1y_{11}}{4}\right]^2 + \left[-2y_5 - 2\mu y_{11} + \frac{\eta\mu}{4}y_1^2 - \left(\frac{h}{R}\right)\frac{\mu y_1y_9}{4}\right]^2$$

$$+ \left(\frac{h}{R}\right)^2\left(-\frac{\mu y_1y_{13}}{2} + \frac{\mu y_1y_{11}}{4}\right)^2 + \frac{1}{8}\left(\frac{h}{R}\right)^2\mu^2y_1^2y_{11}^2\Bigg] + \frac{\eta^2\mu^4}{12}y_1^2$$

$$+ \frac{1}{12}\left\{+\left[-\eta y_1 + \left(\frac{h}{R}\right)y_9\right]^2 + \left(\frac{h}{R}\right)^2 4y_{11}^2 + 8\left(\frac{h}{R}\right)^2 y_{13}^2\right\}$$

$$+ \frac{\nu}{6}\left\{+\mu^2\eta^2y_1^2 - \left(\frac{h}{R}\right)\eta\mu^2y_1y_9\right\} + \frac{(1-\nu)}{24}\left\{+\left[+2\mu\eta y_1 - \left(\frac{h}{R}\right)\mu y_9\right]^2\right.$$

$$\left.+ \left(\frac{h}{R}\right)^2\mu^2 4y_{11}^2\right\} + (1-\nu^2)\left(\frac{\rho c^2}{E}\right)\left\{\left(\frac{dy_1}{d\tau}\right)^2 + \left(\frac{h}{R}\right)\frac{1}{\eta}\left[+\left(\frac{dy_3}{d\tau}\right)^2\right.\right.$$

$$\left.\left.+ \left(\frac{dy_5}{d\tau}\right)^2 + \left(\frac{dy_7}{d\tau}\right)^2 + \left(\frac{dy_9}{d\tau}\right)^2 + 2\left(\frac{dy_{11}}{d\tau}\right)^2 + 2\left(\frac{dy_{13}}{d\tau}\right)^2\right]\right\}\Bigg\} \qquad (79)$$

The application of the variational principle relative to $y_1(\tau)$, $y_3(\tau)$, $y_5(\tau)$, $y_7(\tau)$, $y_9(\tau)$, $y_{11}(\tau)$, and $y_{13}(\tau)$ yields seven Euler equations. The following changes of variables are now employed:

$$\left.\begin{aligned} \frac{dy_1}{d\tau} &= y_2 \quad , \quad \frac{dy_9}{d\tau} = y_{10} \\ \frac{dy_3}{d\tau} &= y_4 \quad , \quad \frac{dy_{11}}{d\tau} = y_{12} \\ \frac{dy_5}{d\tau} &= y_6 \quad , \quad \frac{dy_{13}}{d\tau} = y_{14} \\ \frac{dy_7}{d\tau} &= y_8 \end{aligned}\right\} \tag{80}$$

Next, the seven second-order differential equations (in the independent variable τ) are transformed to fourteen first-order differential equations. The first seven of the fourteen equations are given by Equation (80). The remaining seven equations are

$$\begin{aligned} \frac{dy_2}{d\tau} = &-\left(\frac{E}{\rho c^2}\right)\frac{1}{2(1-\nu^2)}\left\{-\frac{\eta\mu^3 y_1}{2}\left(+2y_5 - \frac{\eta}{8}\mu y_1^2\right) - 2\mu^3\eta y_1 y_7\right. \\ &+ \frac{\mu^4\eta^2}{2}y_1^3 + 3\left[+\frac{\eta}{8}y_1^2 - \left(\frac{h}{R}\right)\frac{y_1 y_9}{4}\right]\left[+\eta y_1 - \left(\frac{h}{R}\right)y_9\right] \\ &+ \left[+2y_{13} - \frac{\eta}{8}y_1^2 + \left(\frac{h}{R}\right)\frac{y_1 y_9}{4}\right]\left[-\eta y_1 + \left(\frac{h}{R}\right)y_9\right] + \frac{3}{8}\left(\frac{h}{R}\right)^2 y_1 y_{11}^2 \\ &+ \frac{1}{2}\left[+2y_{11} - \frac{\eta}{8}y_1^2 + \left(\frac{h}{R}\right)\frac{y_1 y_9}{4}\right]\left[-\eta y_1 + \left(\frac{h}{R}\right)y_9\right] \\ &\left. - 2\left[+y_9 - y_1 - \left(\frac{h}{R}\right)\frac{y_1 y_{11}}{4} - \left(\frac{h}{R}\right)\frac{y_1 y_{13}}{2}\right]\left[+1 + \left(\frac{h}{R}\right)\frac{y_{11}}{4}\right.\right. \end{aligned}$$

(Continued)

$$+ \frac{1}{2}\left(\frac{h}{R}\right) y_{13}\Big] + \frac{1}{2}\left(\frac{h}{R}\right)^2 y_1 y_{11} y_{13} + \frac{1}{2}\left(\frac{h}{R}\right)^2 y_1 y_{13}^2$$

$$- 2\eta\mu y_3\left[1 + \left(\frac{h}{R}\right)\frac{y_{11}}{4} + \left(\frac{h}{R}\right)\frac{y_{13}}{2}\right] + 2\nu\left[+ 2\mu y_5 - \frac{\eta}{8}\mu^2 y_1^2\right]\times$$

$$\left[-\frac{\eta}{4} y_1 + \left(\frac{h}{R}\right)\frac{y_9}{4}\right] - \frac{\eta\nu}{2}\mu^2 y_1\left[+ 2y_{11} - \frac{\eta}{8} y_1^2 + \left(\frac{h}{R}\right)\frac{y_1 y_9}{4}\right]$$

$$+ \nu\mu\left[+ 2y_7 - \frac{\eta}{8}\mu y_1^2\right]\left[+ \eta y_1 - \left(\frac{h}{R}\right) y_9\right]$$

$$- \nu\eta\mu^2 y_1\left[+ \frac{\eta}{8} y_1^2 - \left(\frac{h}{R}\right)\frac{y_1 y_9}{4}\right] + \frac{\eta\mu^2\nu}{2}\left[+ 4y_1 y_{13} - \frac{\eta}{2} y_1^3 + \frac{3}{4}\left(\frac{h}{R}\right) y_1^2 y_9\right]$$

$$+ \nu\eta\mu^2\left[+ \frac{\eta}{2} y_1^3 - \frac{3}{4}\left(\frac{h}{R}\right) y_1 y_9\right] + (1-\nu)\left[- y_3 - \mu y_9 - \left(\frac{h}{R}\right)\frac{\mu y_1 y_{13}}{2}\right.$$

$$\left. + \left(\frac{h}{R}\right)\frac{\mu y_1 y_{11}}{4}\right]\left[-\left(\frac{h}{R}\right)\frac{\mu y_{13}}{2} + \left(\frac{h}{R}\right)\frac{\mu y_{11}}{4}\right] + (1-\nu)\left[- 2y_5 - 2\mu y_{11}\right.$$

$$\left. + \frac{\eta\mu y_1^2}{4} - \left(\frac{h}{R}\right)\frac{\mu y_1 y_9}{4}\right]\left[+ \frac{\eta}{2}\mu y_1 - \left(\frac{h}{R}\right)\frac{\mu y_9}{4}\right] + (1-\nu)\left(\frac{h}{R}\right)^2\left[- \frac{\mu y_1 y_{13}}{2}\right.$$

$$\left. + \frac{\mu y_1 y_{11}}{4}\right]\left[- \frac{\mu y_{13}}{2} + \frac{\mu y_{11}}{4}\right] + \frac{(1-\nu)}{8}\left(\frac{h}{R}\right)^2 \mu^2 y_1 y_{11}^2 + \frac{\eta^2\mu^4}{6} y_1$$

$$- \frac{\eta}{6}\left[- \eta y_1 + \left(\frac{h}{R}\right) y_9\right] + \frac{\nu}{6}\left[+ 2\mu^2\eta^2 y_1 - \left(\frac{h}{R}\right)\eta\mu^2 y_9\right]$$

$$\left. + \frac{(1-\nu)}{6}\eta\mu\left[+ 2\mu\eta y_1 - \left(\frac{h}{R}\right)\mu y_9\right]\right\} \qquad (81)$$

$$\frac{dy_4}{d\tau} = -\left(\frac{E}{\rho c^2}\right)\frac{1}{2(1-\nu^2)}\, n^2 \left\{ + 2\mu^2 y_3 + 2\nu\mu \left[+ y_9 - y_1 - \left(\frac{h}{R}\right)\frac{y_1 y_{11}}{4} \right.\right.$$

$$\left.\left. - \left(\frac{h}{R}\right)\frac{y_1 y_{13}}{2} \right] + (\nu-1)\left[- y_3 - \mu y_9 - \left(\frac{h}{R}\right)\frac{\mu y_1 y_{13}}{2} + \left(\frac{h}{R}\right)\frac{\mu y_1 y_{11}}{4} \right] \right\} \quad (82)$$

$$\frac{dy_6}{d\tau} = -\left(\frac{E}{\rho c^2}\right)\frac{1}{2(1-\nu^2)}\, n^2 \left\{ + 4\mu^2 \left[+ 2y_5 - \frac{\eta\mu}{8} y_1^2 \right] \right.$$

$$+ 4\nu\mu \left[+ 2y_{11} - \frac{\eta}{8} y_1^2 + \left(\frac{h}{R}\right)\frac{y_1 y_9}{4} \right]$$

$$\left. + 2(\nu-1)\left[- 2y_5 - 2\mu y_{11} + \frac{\eta\mu}{4} y_1^2 - \left(\frac{h}{R}\right)\frac{\mu y_1 y_9}{4} \right] \right\} \quad (83)$$

$$\frac{dy_8}{d\tau} = -\left(\frac{E}{\rho c^2}\right)\frac{1}{2(1-\nu^2)}\, n^2 \left\{ - 3\left(\frac{h}{R}\right) y_1 \left[+ \frac{\eta}{8} y_1^2 - \left(\frac{h}{R}\right)\frac{y_1 y_9}{4} \right] \right.$$

$$+ \left(\frac{h}{R}\right) y_1 \left[+ 2y_{13} - \frac{\eta}{8} y_1^2 + \left(\frac{h}{R}\right)\frac{y_1 y_9}{4} \right] + \left(\frac{h}{R}\right)\frac{y_1}{2} \left[+ 2y_{11} \right.$$

$$\left. - \frac{\eta}{8} y_1^2 + \left(\frac{h}{R}\right)\frac{y_1 y_9}{4} \right] + 2\left[+ y_9 - y_1 - \left(\frac{h}{R}\right)\frac{y_1 y_{11}}{4} - \left(\frac{h}{R}\right)\frac{y_1 y_{13}}{2} \right]$$

$$+ 2\nu\mu y_3 + \frac{\nu}{2}\left(\frac{h}{R}\right) y_1 \left(+ 2\mu y_5 - \frac{\eta}{8}\mu^2 y_1^2 \right) - 2\nu\mu \left(\frac{h}{R}\right) y_1 y_7$$

$$- \mu(1-\nu)\left[- y_3 - \mu y_9 - \left(\frac{h}{R}\right)\frac{\mu y_1 y_{13}}{2} + \left(\frac{h}{R}\right)\frac{\mu y_1 y_{11}}{4} \right]$$

$$- \frac{\mu y_1}{4}\left(\frac{h}{R}\right)(1-\nu)\left[- 2y_5 - 2\mu y_{11} + \frac{\eta}{4}\mu y_1^2 - \left(\frac{h}{R}\right)\frac{\mu y_1 y_9}{4} \right]$$

(Continued)

$$+\frac{1}{6}\left(\frac{h}{R}\right)\left[-\eta y_1+\left(\frac{h}{R}\right)y_9\right]-\frac{\nu}{6}\left(\frac{h}{R}\right)\eta\mu^2 y_1-\frac{(1-\nu)}{12}\mu\left(\frac{h}{R}\right)\left[+2\mu\eta y_1\right.$$

$$\left.-\left(\frac{h}{R}\right)\mu y_9\right]\Bigg\} \tag{84}$$

$$\frac{dy_{10}}{d\tau}=-\left(\frac{E}{\rho c^2}\right)\frac{1}{2(1-\nu^2)}\,n^2\left\{+\frac{3}{8}\left(\frac{h}{R}\right)^2 y_1^2 y_{11}+4\left[+2y_{11}\right.\right.$$

$$-\frac{\eta}{8}y_1^2+\left(\frac{h}{R}\right)\frac{y_1y_9}{4}\Big]-\frac{1}{2}\left(\frac{h}{R}\right)y_1\left[+y_9-y_1-\left(\frac{h}{R}\right)\frac{y_1y_{11}}{4}-\left(\frac{h}{R}\right)\frac{y_1y_{13}}{2}\right.$$

$$+\frac{1}{4}\left(\frac{h}{R}\right)^2 y_1^2y_{13}-\frac{\nu}{2}\mu\left(\frac{h}{R}\right)y_1y_3+4\nu\left[+2\mu y_5-\frac{\eta}{8}\mu^2y_1^2\right]$$

$$+\frac{(1-\nu)}{4}\left(\frac{h}{R}\right)\mu y_1\left[-y_3-\mu y_9-\left(\frac{h}{R}\right)\frac{\mu y_1y_{13}}{2}+\left(\frac{h}{R}\right)\frac{\mu y_1y_{11}}{4}\right]$$

$$-2\mu(1-\nu)\left[-2y_5-2\mu y_{11}+\frac{\eta\mu}{4}y_1^2-\left(\frac{h}{R}\right)\frac{\mu y_1y_9}{4}\right]$$

$$+\frac{\mu^2}{4}\left(\frac{h}{R}\right)^2(1-\nu)\left[-\frac{y_1^2y_{13}}{2}+\frac{y_1^2y_{11}}{4}\right]+\frac{(1-\nu)}{8}\left(\frac{h}{R}\right)^2\mu^2y_1^2y_{11}+\frac{2}{3}\left(\frac{h}{R}\right)^2y_{11}$$

$$\left.+\frac{(1-\nu)}{3}\left(\frac{h}{R}\right)^2\mu^2y_{11}\right\} \tag{85}$$

$$\frac{dy_{12}}{d\tau}=-\left(\frac{E}{\rho c^2}\right)\frac{1}{4(1-\nu^2)}\,n^2\left\{+\left(+16\mu^2y_7-\eta\mu^3y_1^2\right)+8\nu\mu\left[+\frac{\eta}{8}y_1^2-\left(\frac{h}{R}\right)\frac{y_1y_9}{4}\right]\right\}$$

(86)

and

$$\frac{dy_{14}}{d\tau} = -\left(\frac{E}{\rho c^2}\right)\frac{1}{4(1-\nu^2)}\, n^2 \left\{+8\left[+2y_{13} - \frac{\eta}{8}y_1^2 + \left(\frac{h}{R}\right)\frac{y_1 y_9}{4}\right]\right.$$

$$-\left(\frac{h}{R}\right)y_1\left[+y_9 - y_1 - \left(\frac{h}{R}\right)\frac{y_1 y_{11}}{4} - \left(\frac{h}{R}\right)\frac{y_1 y_{13}}{2}\right]$$

$$+\frac{1}{4}\left(\frac{h}{R}\right)^2 y_1^2 y_{11} + \frac{1}{2}\left(\frac{h}{R}\right)^2 y_1^2 y_{13} - \nu\mu\left(\frac{h}{R}\right)y_1 y_3 + \nu\eta\mu^2 y_1^2$$

$$-\frac{(1-\nu)}{2}\mu y_1\left[-y_3 - \mu y_9 - \left(\frac{h}{R}\right)\frac{\mu y_1 y_{13}}{2} + \left(\frac{h}{R}\right)\frac{\mu y_1 y_{11}}{4}\right]$$

$$\left.-\frac{(1-\nu)}{2}\left(\frac{h}{R}\right)^2 \mu^2 y_1^2\left[-\frac{y_{13}}{2} + \frac{y_{11}}{4}\right] + \frac{4}{3}\left(\frac{h}{R}\right)^2 y_{13}\right\} \qquad (87)$$

Solution of the 14 coupled differential equations was carried out by standard numerical techniques in conjunction with utilization of the Burroughs 5500 computer in the Stanford University Computation Center.

Unclassified

Security Classification

DOCUMENT CONTROL DATA - R & D

(Security classification of title, body of abstract and indexing annotation must be entered when the overall report is classified)

1. ORIGINATING ACTIVITY *(Corporate author)*

Stanford University
Department of Aeronautics and Astronautics
Stanford, California

2a. REPORT SECURITY CLASSIFICATION

Unclassified

2b. GROUP

N/A

3. REPORT TITLE

NONLINEAR FREE VIBRATIONS OF THIN, CIRCULAR CYLINDRICAL SHELLS

4. DESCRIPTIVE NOTES *(Type of report and inclusive dates)*

Final Technical Report

5. AUTHOR(S) *(First name, middle initial, last name)*

Mayers, Jean
Wrenn, Bruce G.

6. REPORT DATE	7a. TOTAL NO. OF PAGES	7b. NO. OF REFS
July 1970	72	22

8a. CONTRACT OR GRANT NO.	9a. ORIGINATOR'S REPORT NUMBER(S)
DA 44-177-AMC-115(T)	
b. PROJECT NO. Task 1F162204A17002	USAAVLABS Technical Report 69-82
c.	9b. OTHER REPORT NO(S) *(Any other numbers that may be assigned this report)*
d.	

10. DISTRIBUTION STATEMENT

This document is subject to special export controls, and each transmittal to foreign governments or foreign nationals may be made only with prior approval of U. S. Army Aviation Materiel Laboratories, Fort Eustis, Virginia 23604.

11. SUPPLEMENTARY NOTES	12. SPONSORING MILITARY ACTIVITY
	U.S. Army Aviation Material Laboratories Fort Eustis, Virginia

13. ABSTRACT

This report presents the results of a study of the influence of higher order and nonlinear effects on the free vibration behavior of thin, circular cylindrical shells. A recent solution utilizing the Karman-Donnell strain-displacement relations is examined and criticized. A new solution is carried out which removes the basis for criticism and discloses the existence of a nonperiodic vibration behavior, a phenomenon heretofore unknown. Further, solutions are obtained using the strain-displacement relations deduced by Sanders and applied, in an appropriately modified manner, by Mayers and Rehfield to the shell post-buckling problem. The effect of the improved strain-displacement relations in predicting the vibration behavior attendant to a modal shape possessing a small number of circumferential waves is assessed, and recommendations are made for directing future effort on the problem.

DD FORM 1 NOV 65 1473

Unclassified

Security Classification

14 KEY WORDS	LINK A		LINK B		LINK C	
	ROLE	WT	ROLE	WT	ROLE	WT
Cylindrical Shells Vibrations						